CHAPTER 5

Photopolymerised Na-AMPS Hydrogels

Synthesis and Properties

5.1 Photopolymerisation [73-77, 83-84]

Photopolymerisation using photoinitiators utilizes non-ionizing radiation for the polymerisation of photoreactive vinyl unsaturated components such as acrylates and methacrylates. Decomposition of the photoinitiator to give free radicals occurs as a result of the absorption of ultraviolet (UV) light energy. These free radicals then initiate the polymerisation. Using light rather than heat to generate the free radicals means that photopolymerisation can be carried out at ambient temperature with less danger that autoacceleration will occur. This is especially true in bulk polymerisation systems.

In the case of synthetic hydrogels, photoinitiation by UV light is now widely recognized as a very useful synthetic tool. Photoinitiation has various advantages over thermal or redox initiation such as being easier to control, more easily convertible into a continuous process, and offering the possibility of combining both polymerisation and sterilisation into one technological step [85]. Wound dressings manufactured by the simultaneous radiation-induced crosslinking and sterilization of hydrophilic polymers were invented by Rosiak et al [86]. This manufacturing process technology has been successfully and widely used in Europe, America and many countries but is still not practiced in Thailand which continues to import biomedical hydrogel products at great expense.

Photopolymerisation requires UV light in the spectral range of 100-400 nm as the energy source for photoinitiator decomposition. UV light can be produced by various commercially available UV lamps. A typical example is a mercury discharge (or vapour) lamp such as that shown below in Figure 5.1.

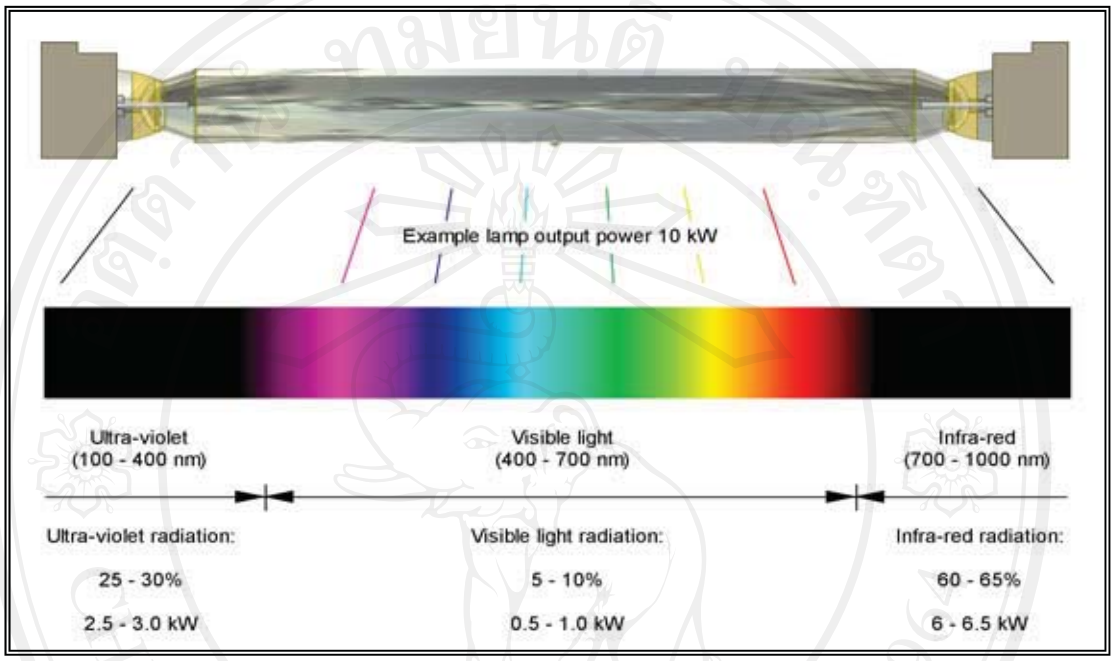

Figure 5.1 : A typical medium pressure mercury discharge lamp power distribution

Amongst the many photoinitiators which are currently available, ***azo compounds*** are well known to be highly efficient. They produce free radicals by dissociation of the C–N bonds either side of the N=N (azo) bond liberating N_2 gas in the process [87]. An example of an azo-type photoinitiator is the 4,4′-azo-bis(4-cyanopentanoic acid) which was used in this work and which decomposes to give free radicals as shown below.

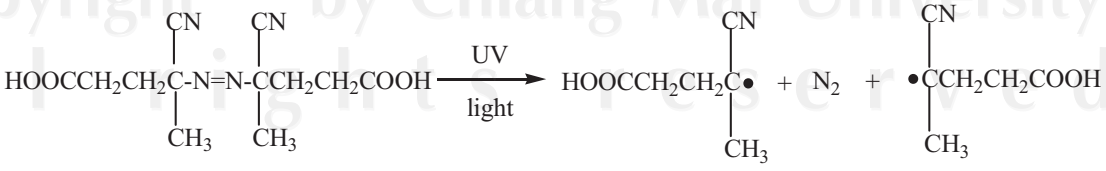

4,4′-azo-bis(4-cyanopentanoic acid)

Another well known type of photoinitiator is the hydroxyphenones. 1-Hydroxycyclohexyl phenyl ketone, commonly known by its trade name of Irgacure 184, is a typical example. This highly efficient photoinitiator, also used in this work, generates free radicals by a unique unimolecular process of light absorption and has absorption peaks at 235-330 nm [88].

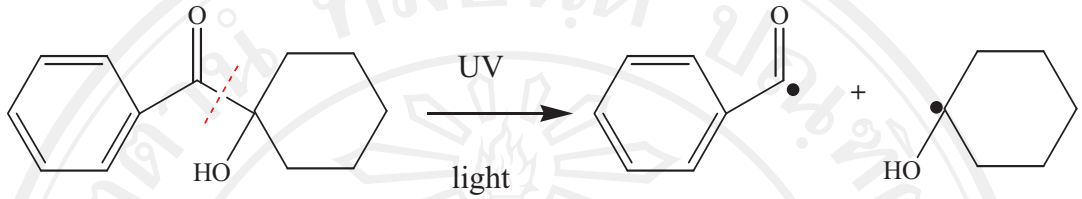

Irgacure 184

Thus, photopolymerisation has many procedural advantages and, as concluded from the results in the previous Chapter 4, is chosen as the preferred method of hydrogel synthesis in this work. However, this is not to say that photopolymerisation is without its limitations. For example, unless thin reaction vessels are employed or the absorption of light is very low, the intensity of the absorbed light, I_a, will vary with the thickness of the reaction system [89]. From the Beer-Lambert Law

$$I = I_0 e^{-\varepsilon[s]\iota}$$

where

I_0 = incident light intensity

I = light incident at a distance ι into the reaction vessel

$[s]$ = concentration of the species s that absorbs light
= [photoinitiator] or [photosensitizer]

ε = molar absorption coefficient of s at the wavelength of absorption

The light intensity absorption, I_a, is then given by

$$I_a = I_0 - I = I_0 (1 - e^{-\varepsilon[s]\iota})$$

where ι now represents the thickness of the reaction vessel.

If l is very small, such as in the applications of photopolymerisation to photolithography and the photocuring of paints, adhesives and inks, then the variation in I_a through the thickness of the film is of negligible importance. However, as thin films increase in thickness to become thin sheets, such as in this work, the variation in I_a with l becomes more significant, leading to a gradient in the photopolymerisation rate, R_p, across the thickness of the sheet. This, in turn, can lead to the setting up of what is referred to as a "polymerisation front" which moves through the thickness of the sheet, thereby concentrating the unreacted monomer into a decreasing surface layer as it proceeds. For a hydrogel wound dressing, this could be problematical but, in commercial practice, any residual monomer at the hydrogel surface tends to be polymerised during the final sterilization step using high-energy gamma-radiation.

Other practical limitations of photopolymerisation include [62]:

(1) Unless light absorption by the photoinitiator occurs above 300-325 nm, quartz reaction vessels need to be used since ordinary glass does not transmit appreciable amounts of energy at wavelengths below 300-325 nm. This limitation has implications for this present work in which an ordinary glass plate was used in the mould construction.

(2) For most monomers, the efficiency of photoinitiation (quantum yield) in bulk is nearly always considerably less than for thermal or redox initiation.

The following sections of this Chapter 5 now describe the effects of the individual components of the Na-AMPS hydrogels on their properties, including a comparison of the 2 photoinitiators mentioned here.

5.2 Na-AMPS Hydrogel Synthesis

As described in the previous Chapter 4, the sequence of operations used in the synthesis of the Na-AMPS hydrogels by photopolymerisation was as shown below.

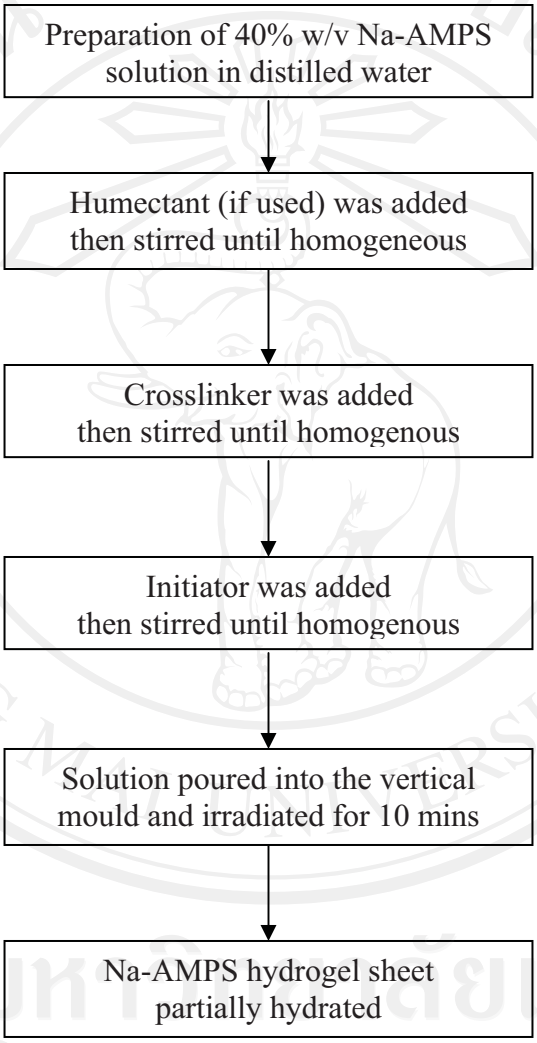

In the context of its application as a wound dressing, the various components used in the preparation of the Na-AMPS hydrogel sheet each fulfil the respective functions described in Table 5.1.

Table 5.1 : The main components used to synthesize the Na-AMPS hydrogel sheets and their respective functions [90].

Components	**Functions**
Monomer (Na-AMPS)	After polymerisation, forms the backbone of the 3-dimensional hydrogel matrix
Humectant (Glycerol)	Reduces the rate of evaporation of water from the hydrogel through hydrogen bonding
Water	Plasticizes the gel allowing it to conform to the site of attachment and enhances the transport of oxygen and active compounds through the matrix
Initiator	Required to initiate polymerisation via the formation of free radicals (in the case of free radical polymerisation)
Crosslinker	Bifunctional monomer/polymer gives a 3-dimensional matrix and the ability for the gel to swell without the loss of structural integrity

5.3 Comparison of Photoinitiator-Crosslinker Systems

5.3.1 Preparation of Hydrogel Sheets

In this work, two different photoinitiator-crosslinker systems, denoted as System I and System II in Table 5.2 and Figure 5.2 below, were compared in the preparation of the Na-AMPS hydrogels.

Table 5.2 : Photoinitiator-crosslinker systems used in hydrogel synthesis.

Usage	System I	System II
Monomer	40% Na-AMPS	40% Na-AMPS
Photoinitiator	4,4′-azo-bis(4-cyanopentanoic acid)	Irgacure 184
Crosslinker	EGDM	Ebecryl 11

Photoinitiator-Crosslinker System I **Photoinitiator-Crosslinker System II**

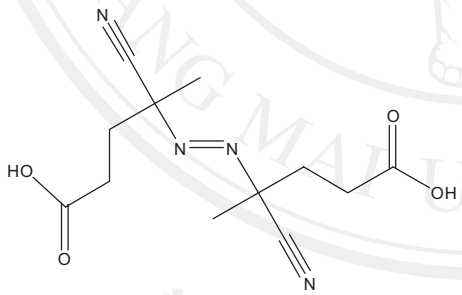

4,4′-azo-bis(4-cyanopentanoic acid) (ACPA)

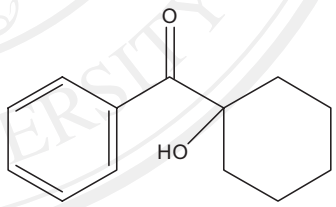

1-hydroxycyclohexyl phenyl ketone (Irgacure 184)

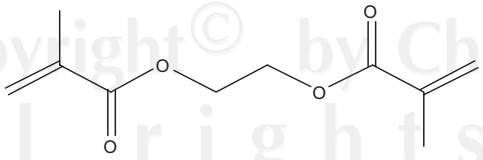

ethylene glycol dimethacrylate (EGDM)

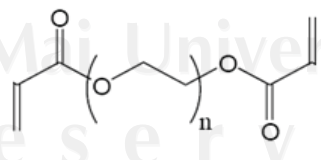

poly(ethylene glycol) diacrylate ($\overline{M}_n \approx 575$) (Ebecryl 11), PEGDA 600

Figure 5.2 : Photoinitiator-crosslinker combinations used in Systems I and II.

In System I, 1.0 mol % of EGDM per mol of Na-AMPS was added into the 40% w/v aqueous Na-AMPS solution as crosslinker together with 0.1 mol % of 4,4'-azo-bis(4-cyanopentanoic acid) (ACPA) as photoinitiator and stirred until a homogeneous solution was obtained. EGDM is a relatively short-length crosslinker in which the crosslink length is equivalent to the length of the —CO–O–CH_2–CH_2–O—CO— unit. This tends to give rather tightly-knit hydrogel networks with limited scope for movement between directly interconnected crosslink points. However, this obviously also depends on the crosslink density.

In System II, Irgacure 184 as photoinitiator was first dissolved in Ebecryl 11 as crosslinker in a w/w ratio of 3:10 to give a homogeneous solution. Then, 0.25% w/v of this solution was added into the 40% w/v Na-AMPS solution and stirred until homogeneous. The difference in mixing procedure from System I was due to the insolubility of Irgacure 184 in aqueous Na-AMPS solution. However, Irgacure 184 was soluble in Ebecryl 11 and the solution was miscible with aqueous Na-AMPS without precipitation. Another notable difference was the structure of the crosslinker. With its constituent PEG chain, $-\left(O–CH_2–CH_2\right)_{\overline{n}}$ ($\overline{n} \approx 10$), Ebecryl 11 is a much longer-length crosslinker than EGDM which would be expected, in theory, to give a looser, more expandable 3-D hydrogel network.

With regard to specific molar concentrations, a 40% w/v (= 40g/100ml) Na-AMPS monomer solution corresponds to a molar monomer concentration of

$$[\text{Na-AMPS}] = \frac{40 \times 1000}{229 \times 100} \text{ M} = 1.75 \text{ M}$$

For System I

[Photoinitiator] = [ACPA] = 0.1% of 1.75 = 0.0018 M

[Crosslinker] = [EGDM] = 1% of 1.75 = 0.0175 M

For System II

$$[\text{Photoinitiator}] = [\text{Irgacure 184}] = \frac{0.25 \times 3 \times 1000}{204 \times 13 \times 100} = 0.0028 \text{ M}$$

$$[\text{Crosslinker}] = [\text{Ebecryl 11}] = \frac{0.25 \times 10 \times 1000}{575 \times 13 \times 100} = 0.0033 \text{ M}$$

The [ACPA] and [EGDM] concentrations in System I were chosen on the basis of giving the best quality hydrogel sheets, as previously described in section 4.2. The [Irgacure 184] and [Ebecryl 11] concentrations in System II were based on typical concentrations given in the patent literature for use in synthesizing hydrogels for biomedical applications [91].

Having prepared the monomer-photoinitiator-crosslinker solutions, photopolymerisation was carried out in a vertical sheet-forming mould at room temperature using a commercially available UV lamp, as previously described in section 3.4. Photopolymerisation was successfully achieved in all cases within 10 mins despite using an ordinary glass plate for the front of the mould facing the lamp. This demonstrated that the UV cut-off of the glass at wavelengths below 300-325 nm was not a problem and that the systems were sufficiently photoreactive to UV light absorption above this limit.

The following section now describes the properties of the hydrogel sheets, in particular those properties relevant to their potential use as a wound dressing.

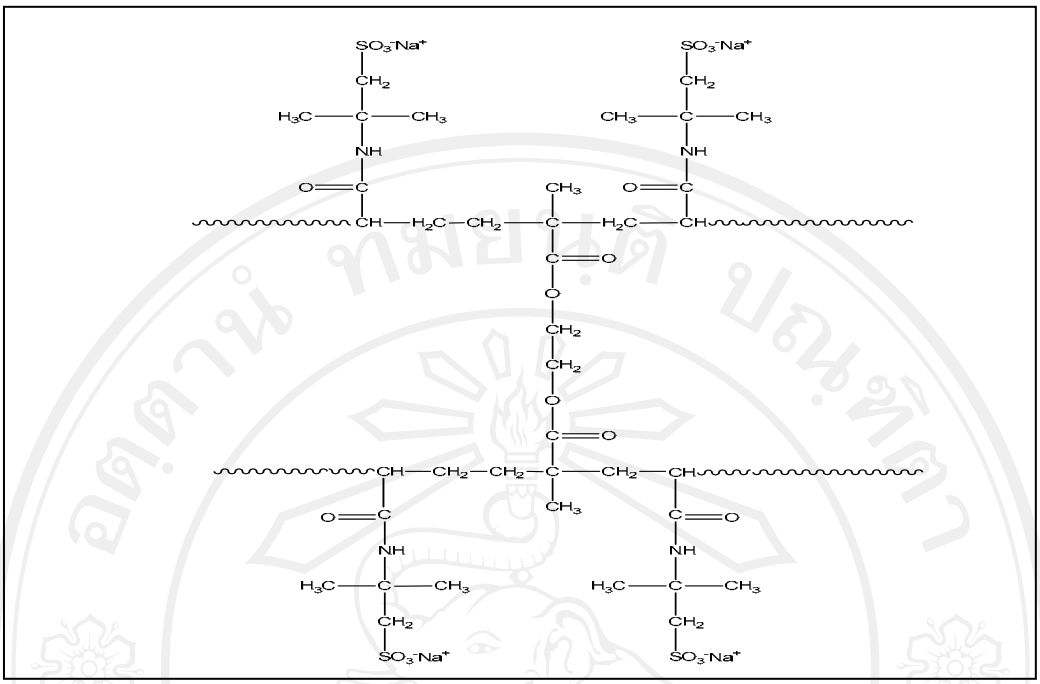

(a) EGDM-crosslinked poly(Na-AMPS)

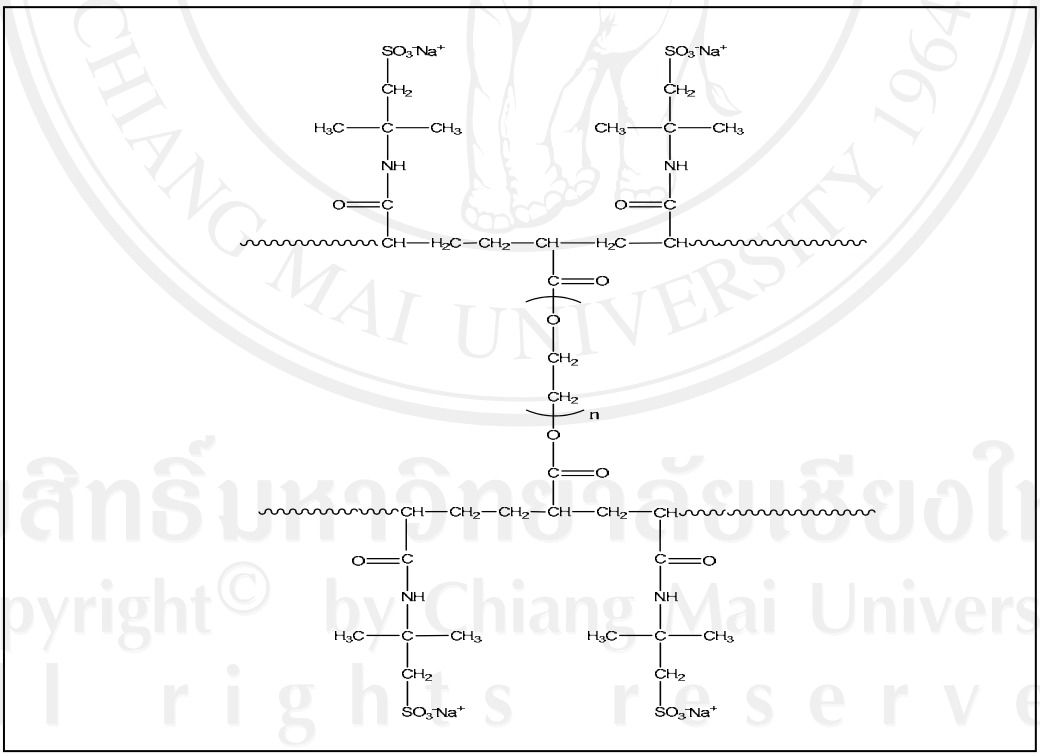

(b) PEGDA-crosslinked poly(Na-AMPS)

Figure 5.3 : Chemical structures showing (a) the EGDM and (b) the PEGDA 600 (Ebecryl 11) crosslinks in poly(Na-AMPS).

5.3.2 Hydrogel Sheet Properties

5.3.2.1 Water Absorption and Retention

The sequence of events used for water absorption and retention testing of the hydrogel sheets is shown in Figure 5.4. Initially, the hydrogel sheets obtained direct from synthesis, having started from an initial Na-AMPS monomer concentration of 40% w/v, had water contents of approximately 60% by wt. Square test samples 1.0 x 1.0 x 0.12 cms in size were then subjected in sequence to:

(1) equilibration to constant weight in air at room temperature (T_{room}) and humidity $\longrightarrow$ equilibrium water content in air = $EWC_{air} \approx$ 25-30 % by wt.

(2) for <u>WATER ABSORPTION</u>, immersion in distilled water at 37±1°C with weight measurements every 1 min for the first 10 mins, then every 2 mins for the next 10 mins, and finally every 5 mins for the next 40 mins $\longrightarrow$ equilibrium water content in water = $EWC_{water} \approx$ 99 % by wt.

(3) for <u>WATER RETENTION</u>, re-equilibration to constant weight in air at room temperature with weight measurements $\longrightarrow$ $EWC_{air} \approx$ 25-30 % by wt.

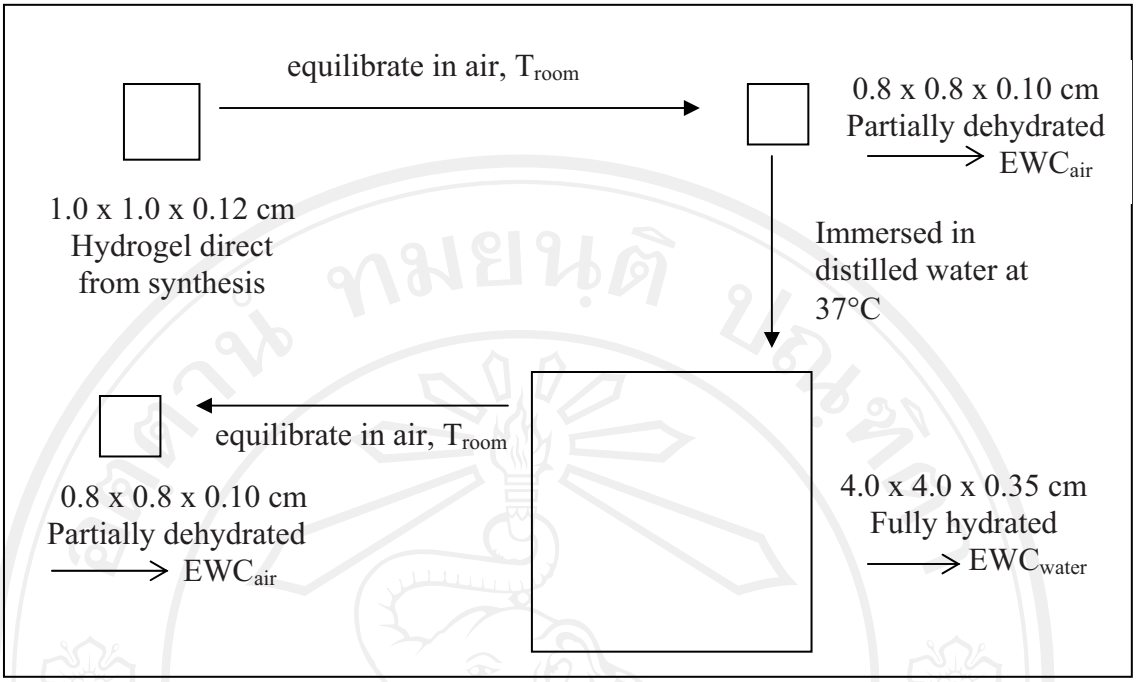

Figure 5.4 : Sequence of events used for water absorption and water retention testing of the hydrogel sheets.

For each weight measurement, the water content (WC) of the sample was calculated using the following expression:

$$WC\,(wt\,\%) = \frac{(w_h - w_d)}{w_h} \times 100\,\% \qquad 5.1$$

where

w_h = hydrated weight of the hydrogel (polymer + water)

w_d = dry weight of the hydrogel (polymer alone)

The value of w_d was obtained by drying the hydrogel sample direct from synthesis to constant (dry) weight in a vacuum oven at 60°C for, typically, about 6 hrs.

For water absorption, the weight measurements and calculated WC values for the System I and System II hydrogels are given in Table 5.3 and the WC-time profiles plotted in Figure 5.5. For water retention, the corresponding data is given in Table 5.4 and Figure 5.7.

Table 5.3 : Water absorption data for 40% w/v Na-AMPS System I and System II hydrogels in distilled water at 37°C.

Time (mins)	SYSTEM I Weight w_h (g)	SYSTEM I WC (%)	Time (mins)	SYSTEM II Weight w_h (g)	SYSTEM II WC (%)
After synthesis			**After synthesis**		
	0.1637	59.80		0.1584	59.97
After equilibration in air ⟶ immersion in distilled water			**After equilibration in air ⟶ immersion in distilled water**		
0*	0.0903	27.13	**0***	0.0849	25.32
1	0.3397	80.63	**1**	0.2640	75.98
2	0.4970	86.76	**2**	0.3622	82.50
3	0.8083	91.86	**3**	0.4812	86.82
4	1.1704	94.38	**4**	0.5645	88.77
6	1.7860	96.32	**6**	0.7505	91.55
8	2.8570	97.70	**8**	1.0422	93.92
10	2.8892	97.72	**10**	1.2543	94.95
12	4.0012	98.36	**12**	1.6583	96.18
14	4.4154	98.51	**14**	1.8214	96.52
16	5.0115	98.69	**16**	2.2475	97.18
18	5.2710	98.75	**18**	2.4578	97.42
20	5.5700	98.82	**20**	2.4795	97.44
25	6.1270	98.93	**25**	2.8627	97.79
30	6.6794	99.01	**30**	3.2098	98.02
35	6.8843	99.04	**35**	3.6148	98.25
40	6.9458	99.05	**40**	4.1283	98.46
45	7.1757	99.08	**45**	4.9939	98.73
50	7.3261	99.10	**50**	5.6923	98.89
55	7.5348	99.13	**55**	6.1332	98.97
60	7.7894	99.16	**60**	6.7328	99.06
DRY**	0.0658	0	**DRY****	0.0634	0

* Starting at EWC_{air}

** Dry weight = w_d (g)

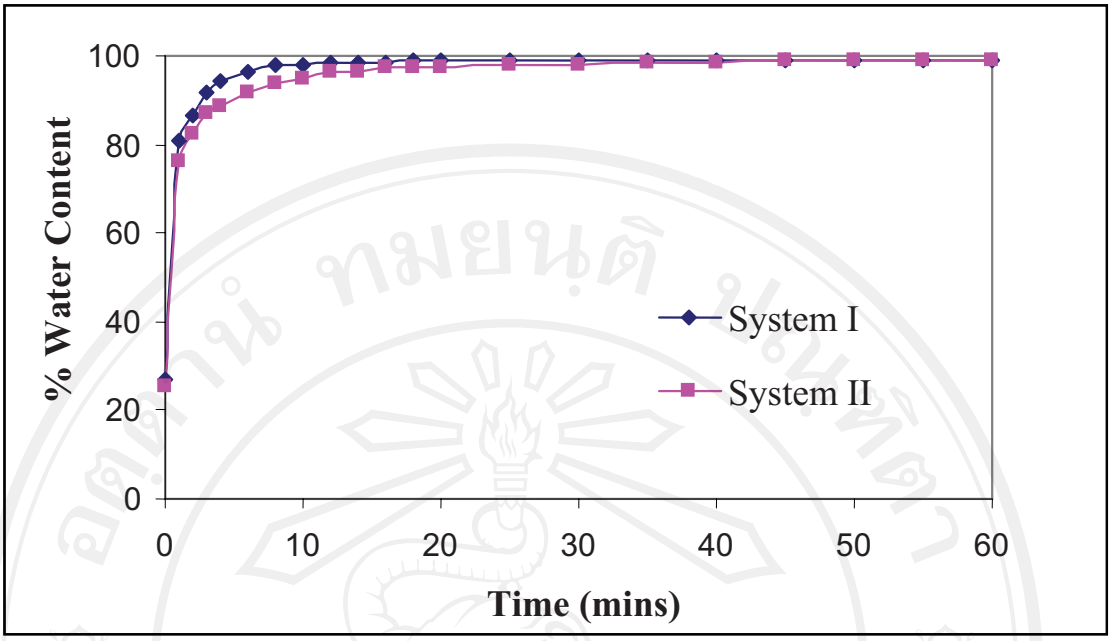

Figure 5.5: Water absorption - time profiles for the 40% w/v Na-AMPS System I and System II hydrogels when immersed in distilled water at 37°C.

As the WC-time profiles in Figure 5.5 show, equilibrium water contents (EWC) of 99% were obtained within 30 mins for both the System I and System II hydrogels. The System I hydrogel showed a slightly faster approach to equilibrium which suggests a slightly looser 3-D network despite its shorter EGDM crosslinker. However, it is not only the crosslink length but also the crosslink density and distribution which are important and so it could be that the System I photoinitiator-crosslinker combination of ACPA-EGDM was less efficient and/or less uniform for crosslinking purposes than the System II combination of Irgacure 184-Ebecryl 11.

The fast approach to equilibrium and the very high EWC are both a reflection of the very strong interaction between water and the Na-AMPS polymer chain. In particular, the sulfonate group, SO_3^-, which is present in each repeating unit, is a relatively large, strongly anionic group which can bind several water molecules. Collectively, the SO_3^- groups therefore exert a strong osmotic effect which draws a lot of water into the hydrogel network quickly before equilibrium is reached within 30 mins. The net result of this is that, in going from $EWC_{air} \longrightarrow EWC_{water}$, the hydrogel swells to about 4 times its original size, as shown in Figure 5.6.

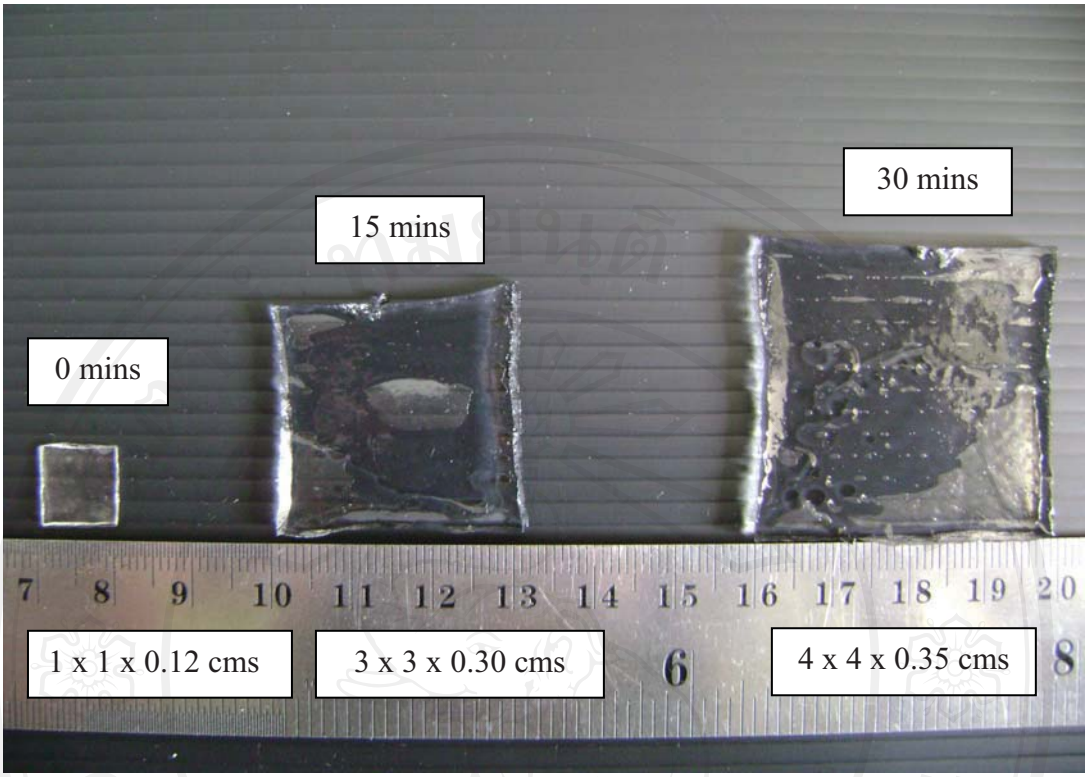

Figure 5.6 : Photographs showing the Na-AMPS hydrogel (System II) at different times of immersion in distilled water at 37°C.

However, in the case of a hydrogel for use as a wound dressing, its ability to release water by evaporation is just as important as its ability to absorb water so that the overall balance of water transport can maintain a moist environment at the wound surface. For water retention in air at room temperature, starting with hydrogel samples at their EWCs in water (EWC_{water}), the weight measurements and calculated WC values for the System I and System II hydrogels are given in Table 5.4 and the WC-time profiles plotted in Figure 5.7.

Table 5.4 : Water retention data for 40% w/v Na-AMPS System I and System II hydrogels in air at room temperature.

Time (mins)	SYSTEM I Weight w_h (g)	SYSTEM I WC (%)	Time (mins)	SYSTEM II Weight w_h (g)	SYSTEM II WC (%)
0 *	7.7894	99.16	0 *	6.7328	99.06
15	4.5672	98.56	15	2.6995	97.65
30	2.6938	97.56	30	1.6484	96.15
45	1.0025	93.44	45	1.0804	94.13
60	0.8461	92.22	60	0.9206	93.11
75	0.3693	82.18	75	0.4102	84.54
90	0.2755	76.12	90	0.2967	78.63
105	0.2184	69.87	105	0.2347	72.99
120	0.1848	64.39	120	0.1835	65.45
135	0.1563	57.90	135	0.1572	59.67
150	0.1269	48.15	150	0.1285	50.66
165	0.1124	41.46	165	0.1105	42.62
180	0.1086	39.41	180	0.1077	41.13
195	0.1022	35.62	195	0.1015	37.54
210	0.0987	33.33	210	0.0978	35.17
225	0.0958	31.31	225	0.0933	32.05
240	0.0922	28.63	240	0.0902	29.71
255	0.0915	28.09	255	0.0882	28.12
270	0.0911	27.77	270	0.0876	27.63
285	0.0909	27.61	285	0.0864	26.62
300	0.0908	27.53	300	0.0859	26.19
315	0.0908	27.53	315	0.0857	26.02
330	0.0907	27.45	330	0.0856	25.93
345	0.0907	27.45	345	0.0855	25.85
360	0.0906	27.37	360	0.0854	25.76
375	0.0906	27.37	375	0.0853	25.67
390	0.0906	27.37	390	0.0853	25.67
405	0.0905	27.29	405	0.0853	25.67
420	0.0904	27.21	420	0.0853	25.67
435	0.0903	27.13	435	0.0853	25.67
600	0.0903	27.13	600	0.0853	25.67
900	0.0903	27.13	900	0.0853	25.67
1200	0.0903	27.13	1200	0.0853	25.67
1440	0.0902	27.05	1440	0.0853	25.67
DRY **	0.0658	0	**DRY ***	0.0634	0

* starting at EWC_{water}

** dry weight of polymer alone = w_d (g)

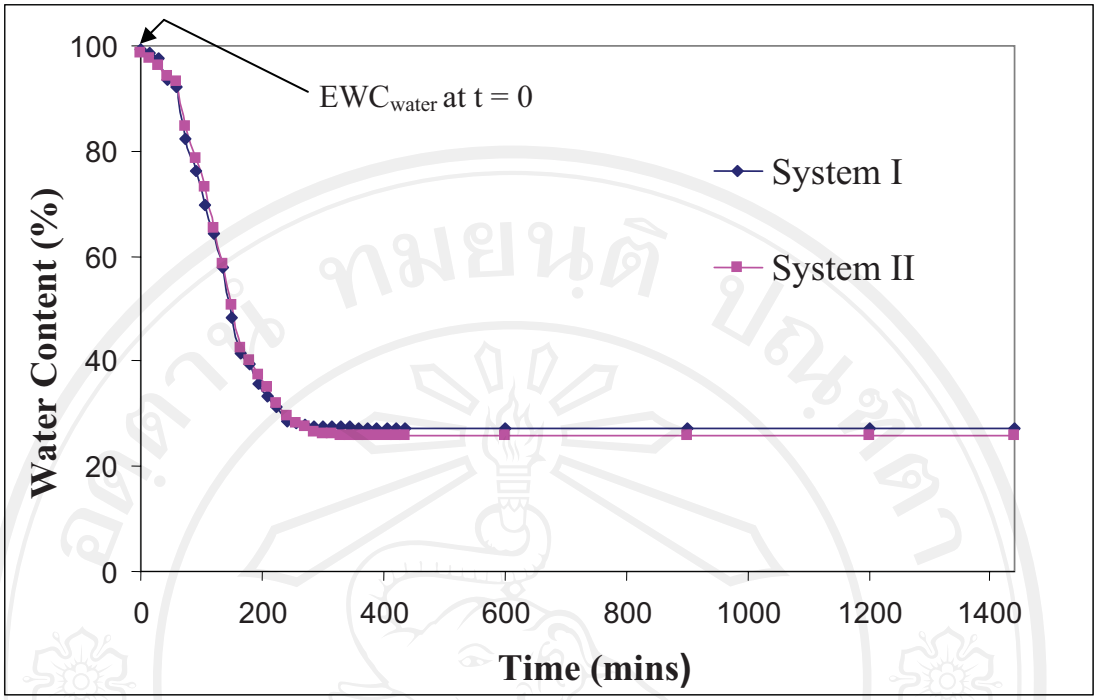

Figure 5.7: Water retention - time profiles for the 40% w/v Na-AMPS System I and System II hydrogels in air at room temperature.

As the results in Figure 5.7 show, the water retention - time profiles for the hydrogels are almost identical. Evaporative water loss takes approximately 4 hrs to reach a constant WC of 26±1% (EWC_{air}) at equilibrium, varying slightly with fluctuations in room temperature (37±2°C) and humidity (50-70%). Apparently, the photoinitiator-crosslinker system has little effect on the water retention – time profile. The most likely explanation for this is that the evaporative water loss from the hydrogels is restricted to the free water (Figure 5.8), the release of which is less polymer structure-dependent than the bound and oriented (semi-bound) water which is retained at equilibrium (EWC_{air}).

Structure of Water in a Crosslinked Hydrogel

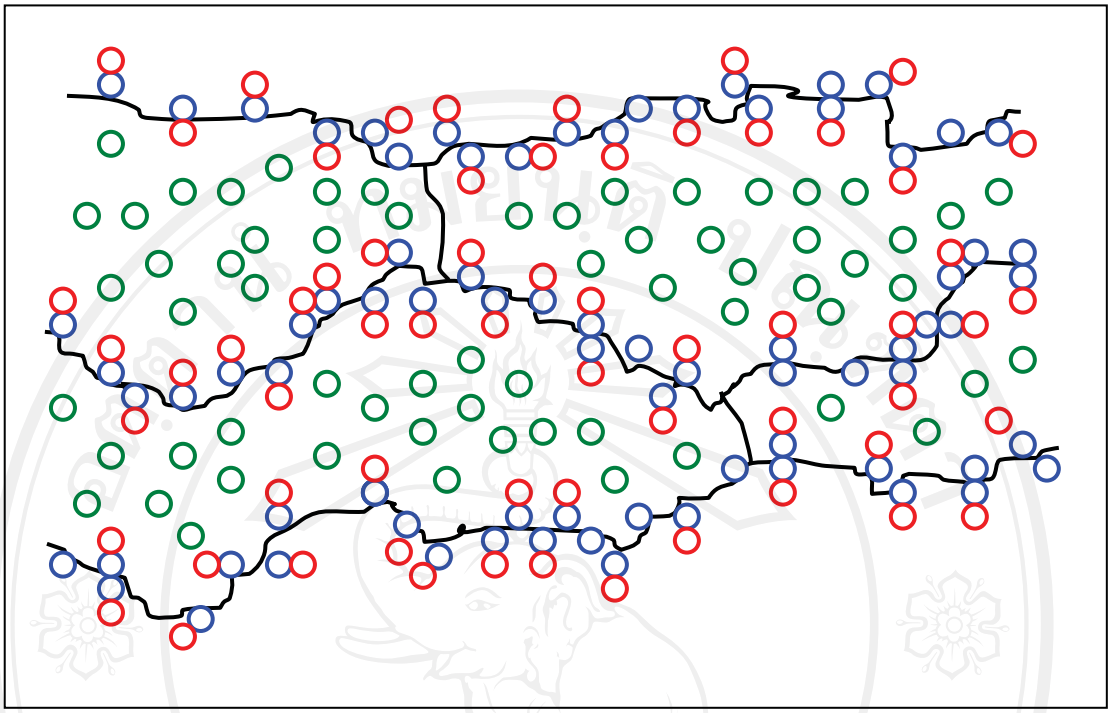

Figure 5.8 : Absorbed water molecules in a 3-D crosslinked hydrogel network.

bound water

oriented water (semi-bound)

free water

where the bound water, when visualized in more detail, may look like

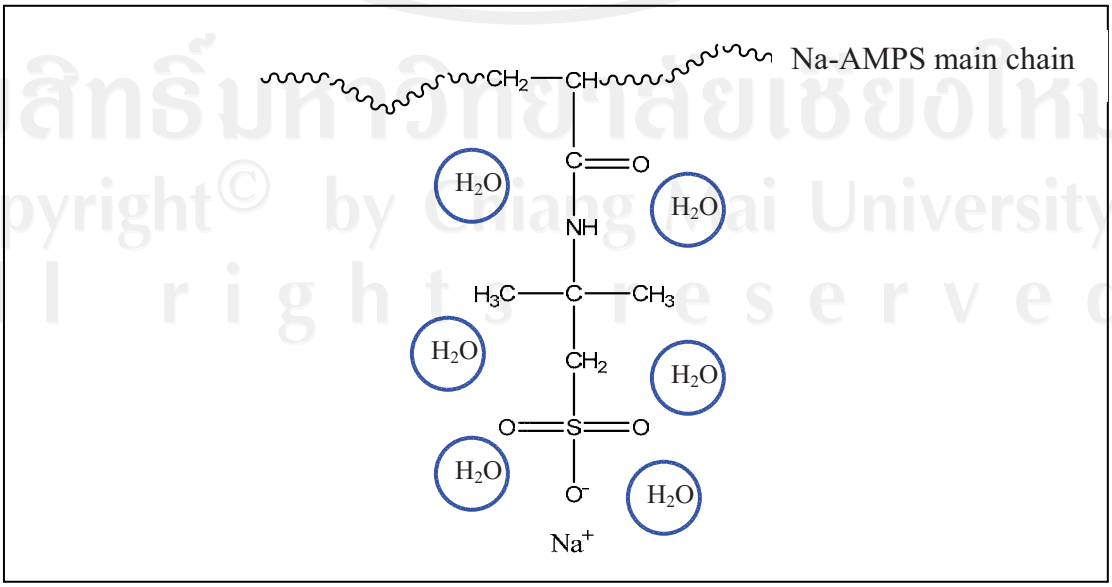

5.3.2.2 Effect of Immersion Medium on Water Absorption

In the previous section, the water absorption properties of the hydrogels in distilled water as the immersion medium was described. However, since the process of water absorption is driven by osmotic pressure, both the amount and rate at which water is absorbed is as dependent on the nature of the immersion medium as it is on the structure of the hydrogel. This is particularly relevant for hydrogels as wound dressings since the wound exudate is a complex mixture of body fluids containing inorganic salts.

Consequently, it was of interest in this work to study the effect of the immersion medium on the water absorption properties of the hydrogels by comparing the previous results in distilled water with those in other water-based media relevant to biomedical applications, namely:

- physiological saline (sodium chloride in water), 0.9% w/v
- synthetic body fluid (SBF)

(a) Saline

Physiological saline was prepared by dissolving 9 g sodium chloride (NaCl) in 1000 ml distilled water (0.9% w/v), similar to the salt concentration in the human body's extracellular fluid. Once prepared, the saline was stored in a refrigerator until required for use.

(b) Synthetic Body Fluid [92-98]

Synthetic body fluid (SBF), first used by Kokubo et al [94], is a metastable aqueous buffer solution of various compounds, mainly inorganic, in concentrations which are approximately equal to those of the inorganic constituents of human blood plasma. The composition of the SBF solution used in this work is given in Table 5.5.

The SBF solution was prepared by dissolving the appropriate quantities of the chemicals listed in Table 5.5 in distilled water. The chemicals were added one by one

with stirring into 700 ml of distilled water in the order given in Table 5.5, allowing each one to dissolve completely before addition of the next. Before addition of the 6th reagent, i.e., $CaCl_2.2H_2O$, 15 ml of 1 M hydrochloric acid (HCl) solution were added to avoid the solution becoming slightly turbid. Following the addition of the final 8th reagent, tris(hydroxymethyl) aminomethane, the solution temperature was raised from ambient to 37 °C and the solution titrated with more 1 M HCl to the physiological pH value of 7.4. During this titration process, the solution was continuously diluted with distilled water to make the final volume equal to exactly 1 L. It was observed in this study that the SBF solution could be stored in a refrigerator at 5°C for one month without any visible signs of precipitation.

Table 5.5 : Chemical composition of the SBF solution used in this work [98].

Order	Chemical	Formula	Amount (g/l)
1	Sodium chloride	NaCl	6.547
2	Sodium bicarbonate	$NaHCO_3$	2.268
3	Potassium chloride	KCl	0.373
4	Disodium hydrogen orthophosphate dihydrate	$Na_2HPO_4.2H_2O$	0.178
5	Magnesium chloride hexahydrate	$MgCl_2.6H_2O$	0.305
6	Calcium chloride dihydrate	$CaCl_2.2H_2O$	0.368
7	Sodium sulphate	Na_2SO_4	0.071
8	Tris(hydroxymethyl) aminomethane	$(CH_2OH)_3CNH_2$	6.057

Water absorption testing of the hydrogels in the saline and SBF media was carried out by the same procedure as that described in the previous section for distilled water. The results are given in Tables 5.6 and 5.7 and the WC-time profiles compared in Figures 5.9-5.12.

As the results in Figures 5.9 and 5.10 show, there was very little difference between the System I and System II WC-time profiles in both saline and SBF. In all 4

cases, the approach to EWC (>90%) was fast and complete within 30 mins indicating that, even in a physiological environment, the hydrogels could be expected to be capable of absorbing large amounts of wound exudate over short periods of time.

Table 5.6 : Weight measurements and WC values for water absorption by the Na-AMPS System I and System II hydrogels in saline at 37°C.

Time (mins)	SYSTEM I		Time (mins)	SYSTEM II	
	Weight w_h (g)	WC (%)		Weight w_h (g)	WC (%)
After synthesis			**After synthesis**		
	0.1968	57.47		0.1985	57.38
After equilibration in air ⟶ immersion in saline			**After equilibration in air ⟶ immersion in saline**		
0 *	0.1082	22.64	**0 ***	0.1113	24.02
1	0.2511	66.67	**1**	0.2756	69.31
2	0.4312	80.59	**2**	0.4169	79.71
3	0.4378	80.88	**3**	0.5265	83.94
4	0.5644	85.17	**4**	0.5763	85.33
5	0.6099	86.28	**5**	0.6286	86.55
6	0.6322	86.76	**6**	0.6877	87.70
8	0.6542	87.21	**8**	0.7470	88.68
10	0.6967	87.99	**10**	0.7644	88.94
12	0.7342	88.60	**12**	0.7942	89.35
14	0.7584	88.96	**14**	0.8241	89.74
16	0.7834	89.32	**16**	0.8407	89.94
18	0.7924	89.44	**18**	0.8862	90.46
20	0.8134	89.71	**20**	0.8920	90.52
25	0.8266	89.87	**25**	0.9042	90.65
30	0.8321	89.94	**30**	0.9144	90.75
35	0.8573	90.24	**35**	0.9295	90.90
40	0.8611	90.28	**40**	0.9301	90.91
45	0.8712	90.39	**45**	0.9412	91.01
50	0.8741	90.42	**50**	0.9534	91.13
55	0.8792	90.48	**55**	0.9632	91.22
60	0.8979	90.68	**60**	0.9796	91.37
DRY **	0.0837	0	**DRY ****	0.0846	0

* starting at EWC_{air}

** dry weight of polymer alone = w_d (g)

Table 5.7 : Weight measurements and WC values for water absorption by the Na-AMPS System I and System II hydrogels in SBF solution at 37°C.

Time (mins)	SYSTEM I Weight w_h (g)	SYSTEM I WC (%)	Time (mins)	SYSTEM II Weight w_h (g)	SYSTEM II WC (%)
After synthesis			**After synthesis**		
	0.1977	57.36		0.1975	58.23
After equilibration in air ⟶ immersion in SBF			**After equilibration in air ⟶ immersion in SBF**		
0 *	0.1088	22.52	**0 ***	0.1058	22.02
1	0.2811	70.01	**1**	0.2756	70.07
2	0.3543	76.21	**2**	0.3690	77.64
3	0.4678	81.98	**3**	0.4565	81.93
4	0.5044	83.29	**4**	0.5023	83.58
5	0.5399	84.39	**5**	0.5846	85.89
6	0.6322	86.67	**6**	0.6582	87.47
8	0.7542	88.82	**8**	0.7342	88.76
10	0.7967	89.42	**10**	0.8064	89.77
12	0.9342	90.98	**12**	0.8551	90.35
14	0.9784	91.38	**14**	0.8994	90.83
16	1.0234	91.76	**16**	0.9943	91.70
18	1.1824	92.87	**18**	1.1073	92.55
20	1.2342	93.17	**20**	1.1892	93.06
25	1.3966	93.96	**25**	1.2412	93.35
30	1.5321	94.50	**30**	1.2644	93.48
35	1.6728	94.96	**35**	1.4952	94.48
40	1.7811	95.27	**40**	1.5081	94.53
45	1.7912	95.29	**45**	1.5127	94.55
50	1.8154	95.36	**50**	1.7554	95.30
55	1.8623	95.47	**55**	1.7632	95.32
60	1.8796	95.52	**60**	1.7796	95.36
DRY **	0.0843	0	**DRY ****	0.0825	0

* starting at EWC_{air}

** dry weight of polymer alone = w_d (g)

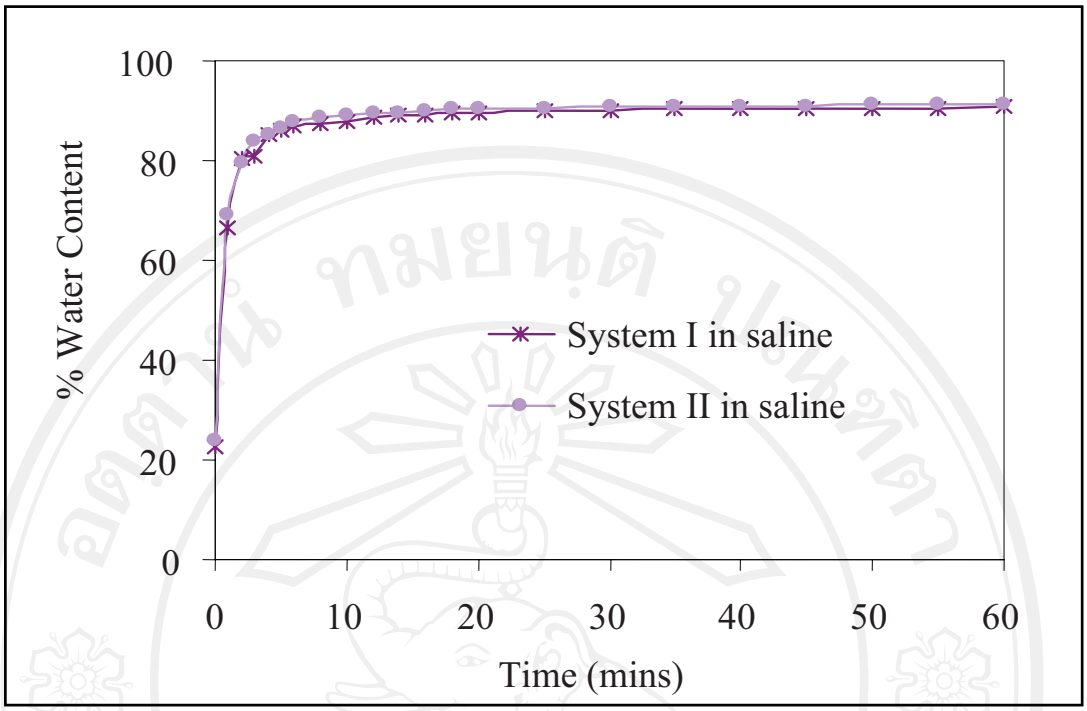

Figure 5.9 : WC-time profiles for water absorption by the 40% w/v Na-AMPS System I and System II hydrogels in saline at 37°C.

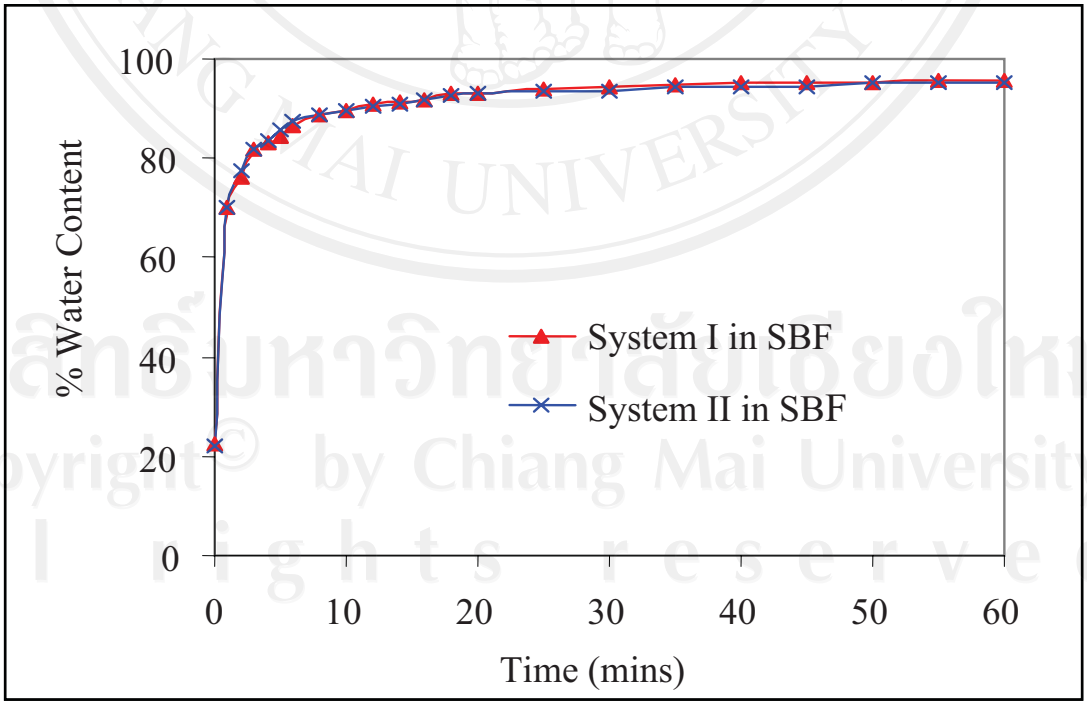

Figure 5.10 : WC-time profiles for water absorption by the 40% w/v Na-AMPS System I and System II hydrogels in SBF solution at 37°C.

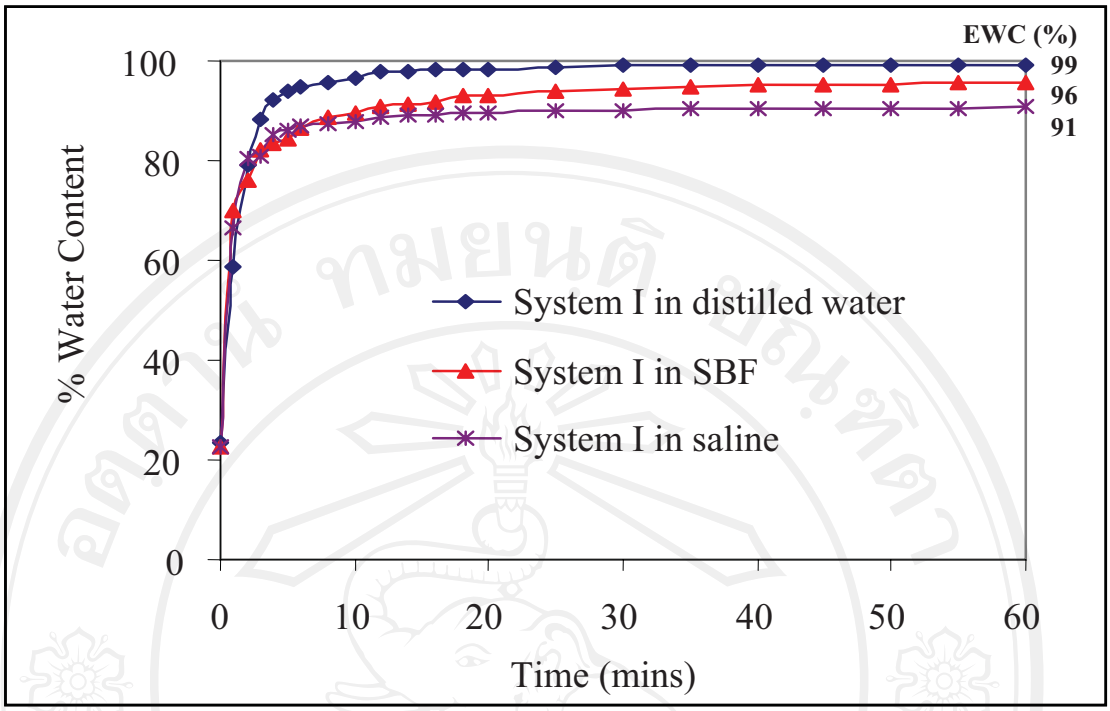

Figure 5.11 : Effect of immersion medium on the WC-time profile for water absorption by the 40% w/v Na-AMPS System I hydrogel at 37°C.

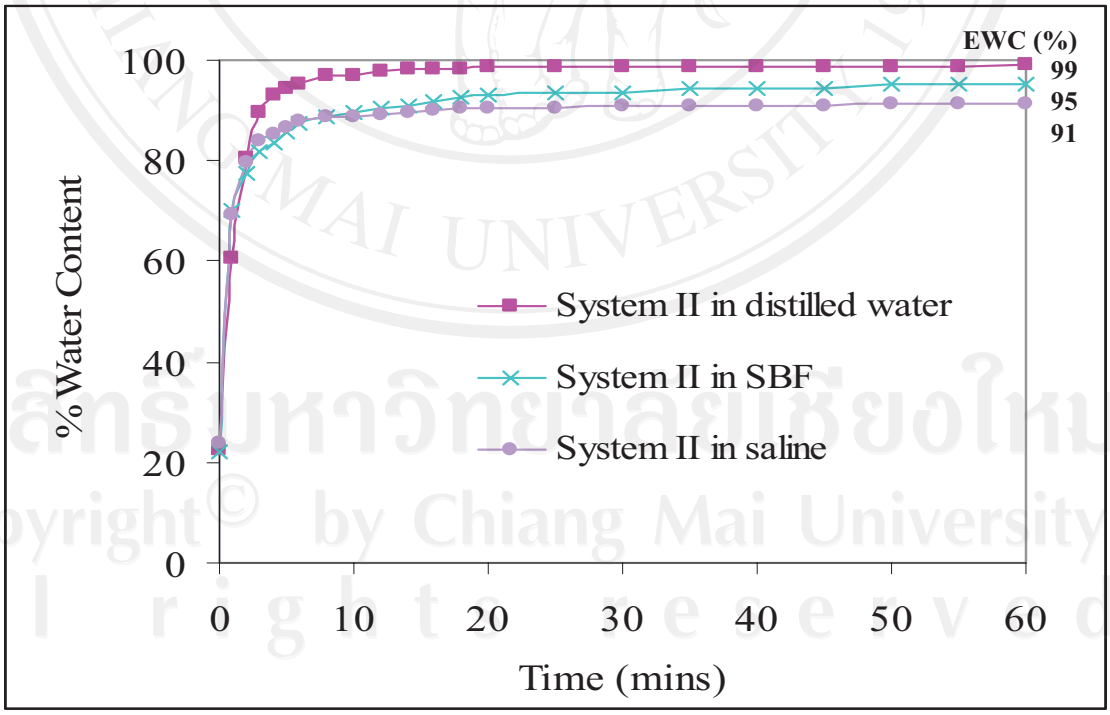

Figure 5.12 : Effect of immersion medium on the WC-time profile for water absorption by the 40% w/v Na-AMPS System II hydrogel at 37°C.

The effect of the immersion medium on the water absorption profiles of the hydrogels is shown in Figures 5.11 and 5.12. The most obvious differences are in the final EWC values which for both hydrogels are in the order:

EWC in : distilled water > SBF > saline

The decreases in the EWCs in saline and SBF relative to distilled water are a result of decreases in the osmotic pressure driving force for water to enter the hydrogel due to the ionic concentrations in saline and SBF. However, these decreases are less than 10% and it is also significant for note that the initial increases in WC during the first 2 mins are just as fast as in distilled water.

It can therefore be concluded that both the saline and SBF media, at their respective ionic concentrations, do not seriously impair the water absorption properties of the Na-AMPS hydrogels. Thus, they could still be expected to be highly efficient at absorbing wound exudate in their physiological use as wound dressings. The EWC values are compared in Table 5.8 below.

Table 5.8 : EWC values for the Na-AMPS System I and II hydrogels in distilled water, saline and SBF solution at 37°C.

Na-AMPS Hydrogel	**EWC (%) in**		
	Distilled Water (± 0.5)	**SBF (± 1.0)**	**Saline (± 1.0)**
System I	99.2	95.5	90.7
System II	98.9	95.4	91.4

5.3.2.3 Water Vapour Transmission [99-103]

The water vapour transmission rates (WVTR) through the hydrogels were measured using the standard ASTM E96-93 (1990) Water Cup Method, as illustrated in Figures 5.13 and 5.14 below.

Figure 5.13 : Photograph of the water cup used for water vapour transmission rate measurements.

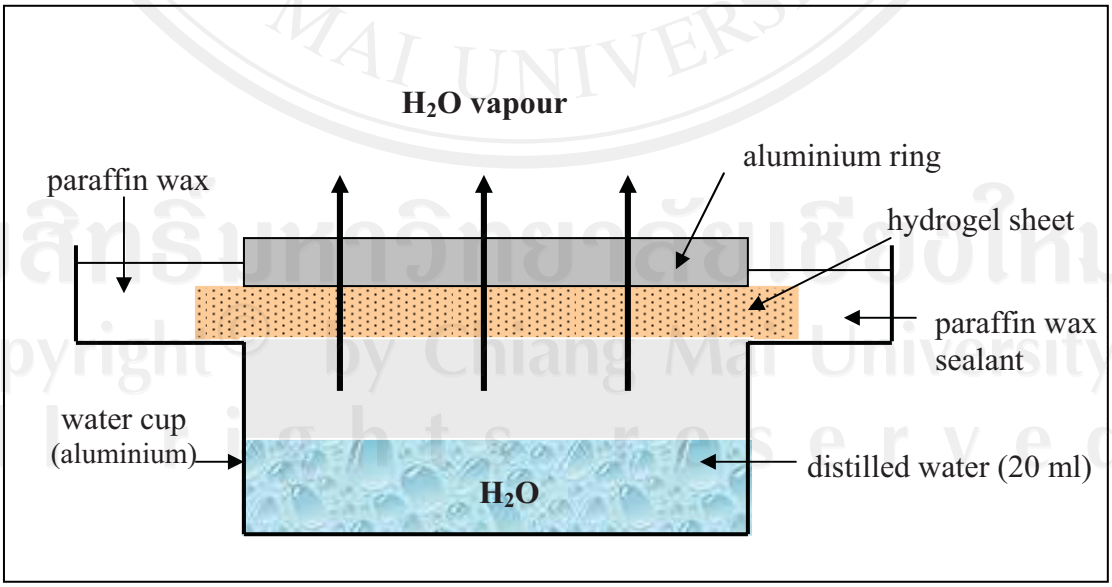

Figure 5.14 : Schematic diagram of the Water Cup Method used for water vapour transmission rate measurements.

For each WVTR determination, the hydrogel was first equilibrated in air to its EWC_{air} and a circular-shaped sample (diameter = 5 cm, thickness = 0.12 cm) cut and placed in position on the water cup. The edges of the sample were sealed with paraffin wax. The cup contained 20 ml of distilled water which maintained a saturated water vapour-filled space below the sample, as shown in Figure 5.14.

The complete water cup assembly was then weighed accurately and placed in an incubator at 37±1°C and relative humidity 55-60%. Weight measurements were made every 30 mins for the first 8 hrs and then intermittently up to a total of 72 hrs. The data obtained is given in Table 5.9 and the weight loss versus time plots shown in Figure 5.15. The timescales of these plots are expanded in Figure 5.16 alongside the corresponding open cup (i.e., no sample) data for comparison. The WVTR rates for the hydrogels are obtained from the linear slopes via the following equation (5.2).

$$WVTR = (G/t) / A \qquad (5.2)$$

WVTR	=	water vapour transmission rate ($g/hr.m^2$)
G	=	weight loss (g)
t	=	time (hrs)
A	=	test area (cup mouth area) = 2.83×10^{-3} m^2
G/t	=	slope of the straight line graph (g/hr)

The expanded plots in Figure 5.16 and the WVTR values for the hydrogels of:

System I	=	101.77 g m^{-2} hr^{-1}	(= 64.00 %)
System II	=	129.33 g m^{-2} hr^{-1}	(= 81.33 %)
cf., Open Cup	=	159.01 g m^{-2} hr^{-1}	(= 100 %)

confirm that the hydrogels can effectively decrease evaporative water loss to a significant extent and thereafter control it at a constant rate. The WVTR is actually a composite rate derived from the interdependent component rates shown in Figure 5.17.

Table 5.9 : Water vapour transmission rate (WVTR) data for the Na-AMPS System I and II hydrogels at 37°C from the Water Cup Method.

Time t (mins)	Weight Loss G (g)		
	SYSTEM I	SYSTEM II	OPEN CUP
0 *	0	0	0
30	0.0970	0.2031	0.1846
60	0.3014	0.3876	0.3839
90	0.4243	0.5198	0.6167
120	0.5627	0.7342	0.8315
150	0.7043	0.9257	1.0327
180	0.8840	1.1405	1.2663
210	1.0421	1.3287	1.4738
240	1.1834	1.5281	1.7504
270	1.3326	1.6654	2.0026
300	1.4747	1.8452	2.2295
330	1.5863	2.0162	2.4136
360	1.7126	2.2125	2.6455
390	1.8761	2.4011	2.8340
420	2.0154	2.5658	3.0843
450	2.1390	2.7499	3.2950
480	2.3295	2.8983	3.5422
1440	5.8546	6.6254	12.2892
1620	6.8778	7.6554	13.2840
1680	7.1220	7.9393	13.6070
1740	7.2612	8.2682	14.3976
2880	11.4662	13.5417	17.8616
4320	17.3026	19.7128	19.0774
SLOPE g/min	0.0048	0.0061	0.0075
WVTR g m^{-2} hr^{-1}	101.77	129.33	159.01

* Hydrogel sample starting at EWC_{air} at t = 0

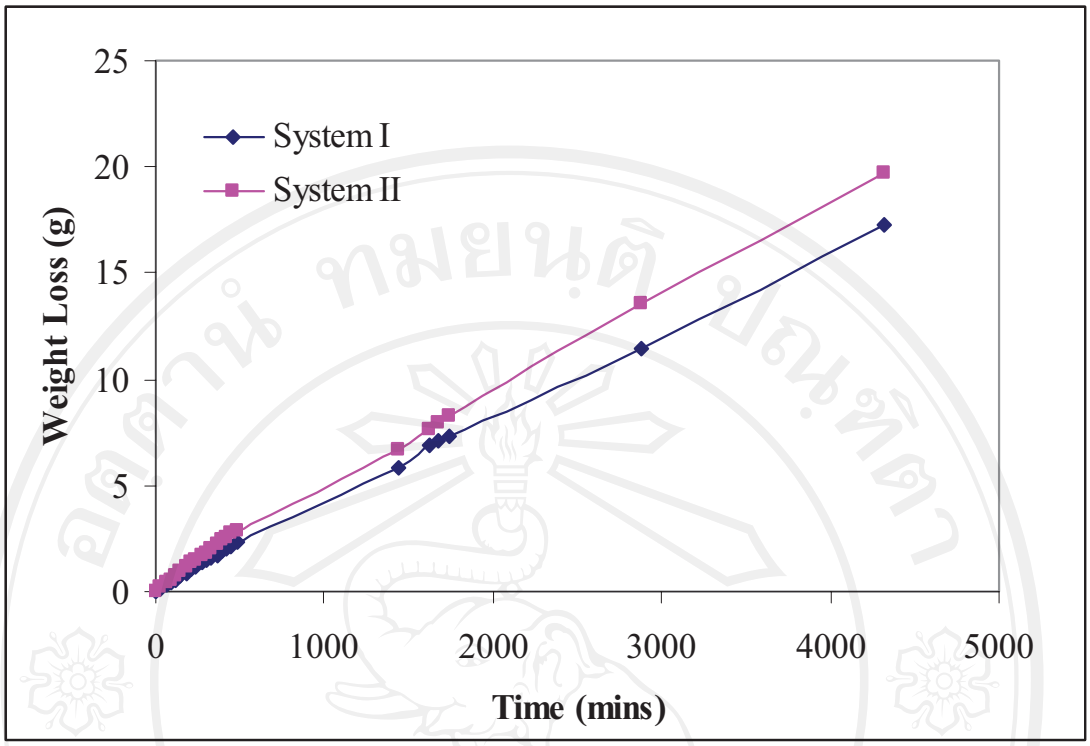

Figure 5.15 : Water vapour transmission - time profiles for the hydrogel sheets at 37°C and 55-60% relative humidity over a 72 hrs time period.

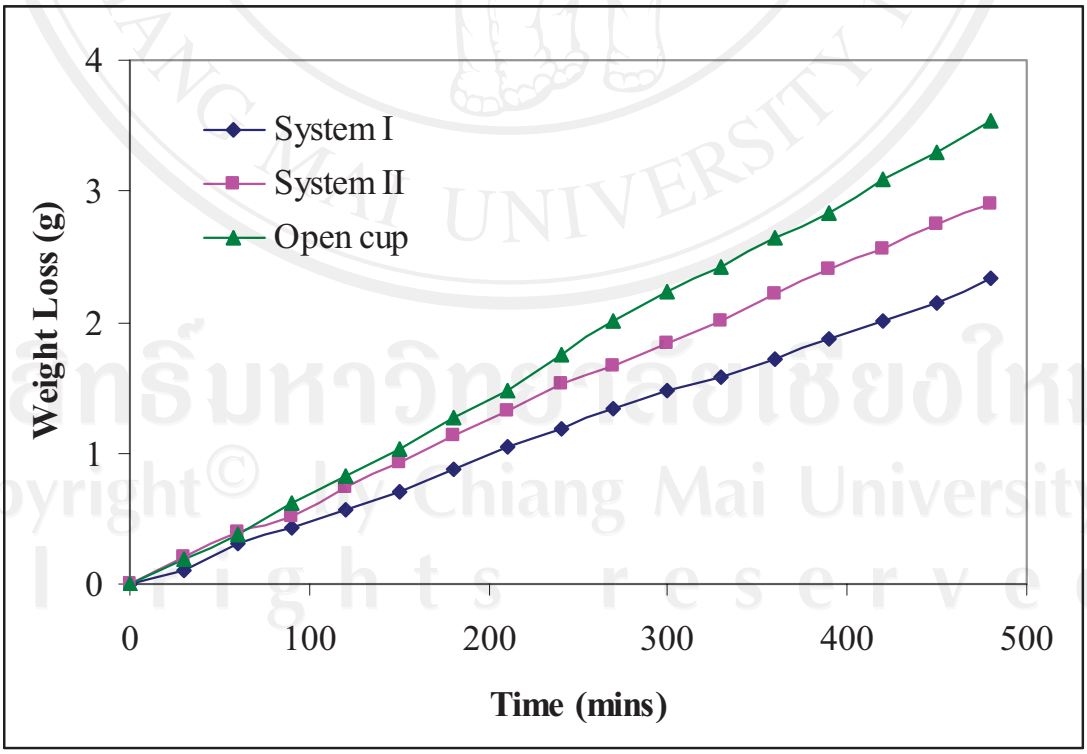

Figure 5.16 : Water vapour transmission plots (expanded time scale) for the hydrogel sheets over the first 8 hrs compared with an open cup (no sample).

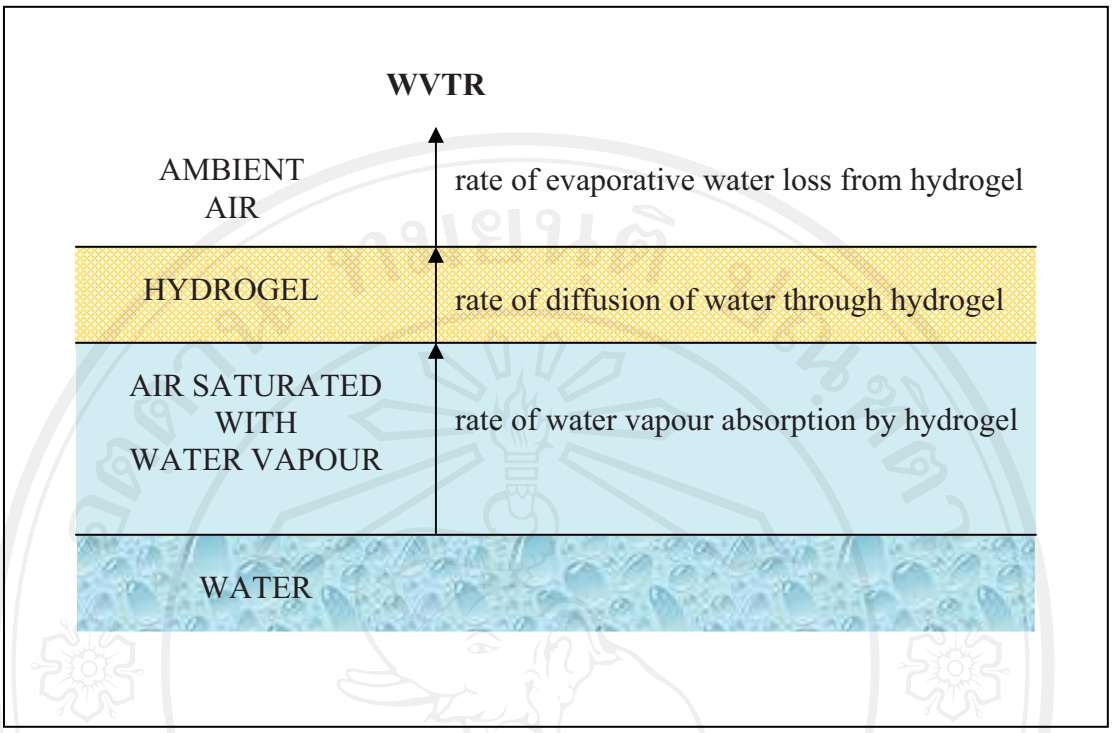

Figure 5.17: Water vapour transmission through a hydrogel broken down into its interdependent component rates.

Thus, water vapour transmission through a hydrogel is seen to be a multivariate process which quickly leads to a constant WVTR. The critical point as far as a hydrogel wound dressing is concerned is that this WVTR is at an appropriate level to control the evaporative water loss from a typical second-degree burn. What this means in practice is that the hydrogel is able to maintain a moist environment at the wound surface which is most conducive to the wound healing process.

In Table 5.10, the WVTR values for the System I and System II hydrogels are compared with those of some commercial wound dressings currently in use. Also included in Table 5.10 are typical rates of evaporative water loss from normal skin and first, second and third-degree burns. The results show that the WVTR values for the hydrogels from this work are within the range of the commercial dressings and significantly less than the rate of evaporative water loss (EWL) from a typical second-degree burn. These are encouraging results bearing in mind that the target WVTR is around midway between the EWL rates from normal skin and a second-degree burn.

As for the difference in WVTR between the System I and II hydrogels in Figure 5.16, this is most likely due to differences in network structure arising from the different photoinitiator/crosslinker combinations used. For example, differences in crosslink length, density and distribution can all affect the extent to which a hydrogel network can expand under hydration, even at the same water content. How this volume expansion affects the WVTR value in the Water Cup Method is difficult to quantify because the equation WVTR = (G/t) / A only takes account of the test area A, not the sample thickness. Therefore, the difference in the WVTR values of the hydrogels could be at least partly due to a difference in sheet thickness at their respective EWCs under the conditions of the test.

Table 5.10: Comparison of the WVTR values for the System I and II hydrogels with those of some commercial wound dressings and typical rates of evaporative water loss from normal skin and first, second and third-degree burns.

DATA SOURCE	SAMPLE / MATERIAL	WVTR g m^{-2} hr^{-1}
THIS WORK	System I hydrogel System II hydrogel Distilled water (open cup)	101.77 ± 5 129.33 ± 5 159.01 ± 5
COMMERCIAL DRESSINGS [102]	Biabrone Metalline OpSite Omiderm	154 53 33 208
PHYSIOLOGICAL DATA* [103]	Normal skin First-degree burn Second-degree burn Third-degree burn	8.5 ± 0.5 11.6 ± 1.1 178.1 ± 5.5 143.2 ± 4.5

* Typical rates of evaporative water loss from an average adult person

5.3.2.4 Peel Strength [104-108]

Peel strength, which in turn is related to substrate adhesion, is obviously an important property for a wound dressing where the substrate is human skin. Therefore, in the development of a wound dressing, it is important to recognise and understand the forces responsible for adhesive bond formation and performance. Generally, a wound dressing has to provide good adhesive and cohesive forces. Surface wettability is important in the formation of an adhesive bond between the adherend and a substrate. Cohesive strength is essential for the successful mechanical transfer of force through the adhesive bond to the substrate. Together these forces affect the ease of application, strength of adhesion and ease of removal of partially hydrated ionic hydrogels from human skin.

Adhesive performance is controlled by a material's properties that together result in good application and extended adhesion characteristics. Techniques that can be employed to measure these properties include tack, peel adhesion and dynamic mechanical measurements such as shear strength.

The skin adhesiveness of partially hydrated hydrogels is dependent on 3 elements that work together to determine the suitability of the hydrogel for use as a wound dressing.

(1) The **rheological** properties of the hydrogel which determine its viscoelastic behaviour
(2) The **hydrophilic** component that removes the lubricating interfacial water layer between the hydrogel and the skin
(3) The **hydrophobic domains** within the hydrogel which interact with the lipids of the skin, thereby contributing to the adhesive bond between the hydrogel and the skin.

Upon removal, most hydrogel wound dressings detach the upper *Stratum corneum* layer after a few seconds of skin contact. This is known as the "stripping effect". As a result, reapplication of the detached dressing is rarely possible and application of a fresh dressing is necessary. The effect of skin damage during removal of the hydrogel is difficult to quantify but is nevertheless an important consideration in the assessment of its suitability as a wound dressing. A schematic diagram showing the detachment of epidermal cells upon removal of any form of adhesive patch is shown in Figure 5.18.

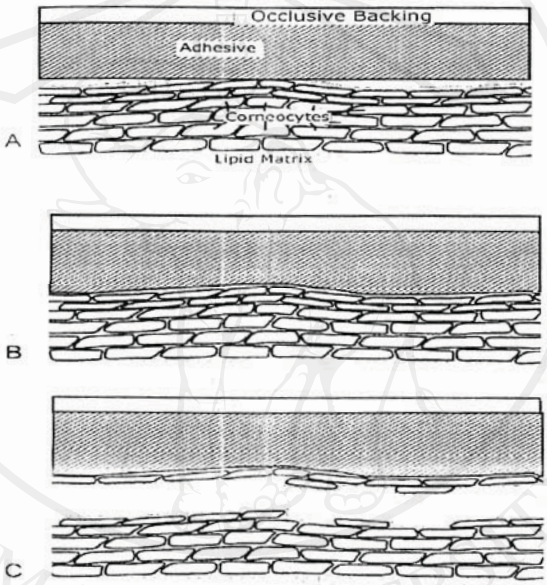

Figure 5.18: Schematic diagram of the detachment of epidermal cells by removal of an adhesive patch [90].

A peel strength test can be used to give an indication of the ease of removal of a hydrogel from a substrate. This gives important information about the strength of adhesion. Peel strength tests also provide information about the relative cohesive strength of the hydrogel and the potential for cohesive failure (tearing) of the hydrogel prior to adhesive failure of the bond between the hydrogel and the substrate. Variables to consider during peel strength testing of a material include contact time and pressure, the nature of the substrate, angle of peel and peel speed.

In general, peel strength tests are carried out by measuring the resistance to the peeling of a material from an artificial substrate rather than human skin. Major differences between these artificial testing surfaces and the human *Stratum corneum* make them poor models and measurements simply provide a comparative indication of the adhesive behaviour of the test sample. However, the shear force required to remove a skin adhesive hydrogel from a substrate can be quantified to some extent using a 90° perpendicular peel test. An instrumental set-up which has been designed for this purpose is shown in Figure 5.19. It consists of a commercial tensile testing machine (Hounsfield Tensometer) and a sliding tray containing the substrate. The substrate used in this work was a sheet of smooth stainless steel encased in a melamine-faced fibre board support allowing a central area to be exposed upon which the hydrogel sample in the form of a rectangular strip was attached.

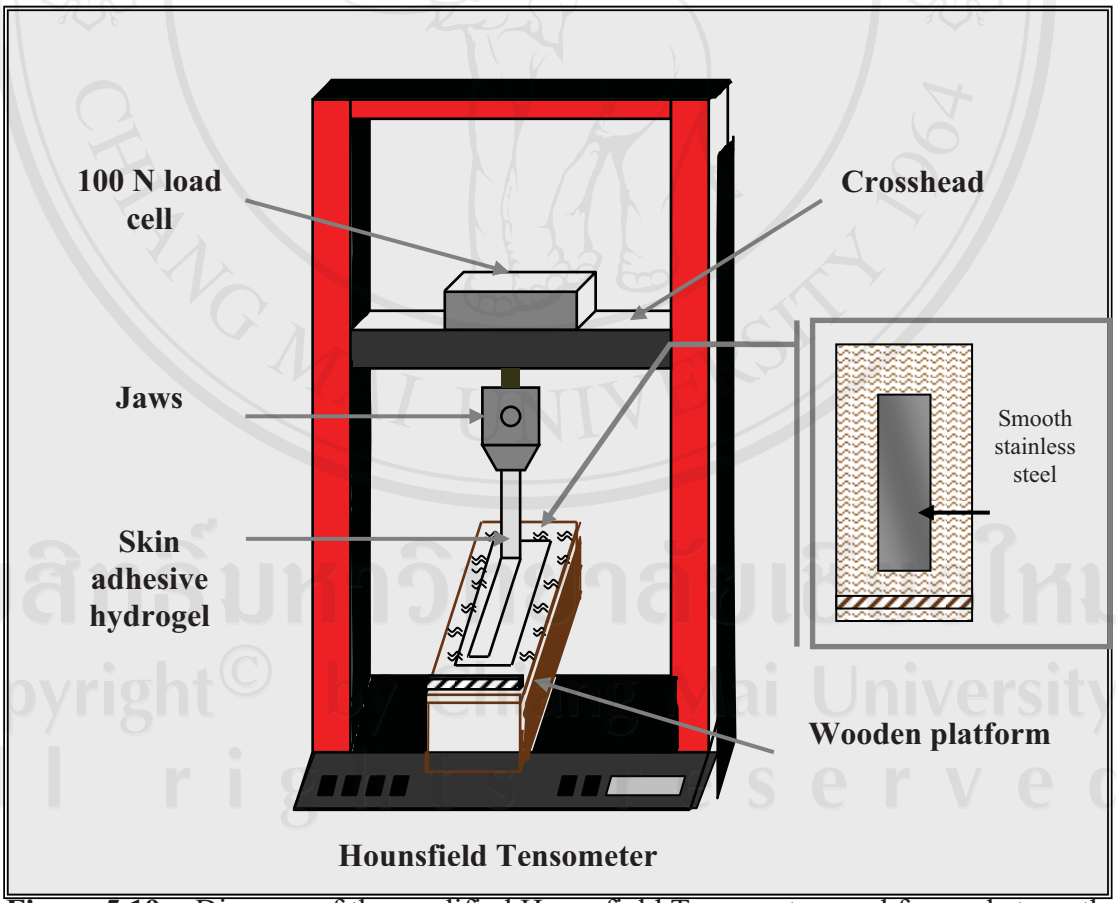

Figure 5.19 : Diagram of the modified Hounsfield Tensometer used for peel strength testing [90].

Test Conditions:

- Crosshead (peel) speed = 500 mm/min
- Sample width = 25 mm
- Sample length = 15 cm
- Sample thickness = 1.20 ± 0.20 mm
- Load cell = 100 N
- Peel angle = 90° (constant)

The peel strength was taken as the shear force required to peel the hydrogel sample from either the stainless steel substrate or human skin (author's forearm).

For each peel strength test, 3 strips of the System I and II hydrogels measuring 15 cm x 2.5 cm and each at their EWC_{air} were tested and the average result recorded. Each strip was pressed gently onto the stainless steel osmall amount or skin substrate leaving a sample that could be clamped in the jaws of the tensometer. The strip was peeled from the substrate at a rate of 500 mm/min as the tray was moved horizontally forward ensuring that the sample removed was at a constant angle of 90°. A 100 N load cell was used for all of the peel tests and the data relayed to the computer software which calculated the peel strength in units of N/25mm for each sample. A typical peel test force-extension trace for the System I hydrogel on the skin substrate is shown in Figure 5.20 from which the peel strength is taken as the maximum force recorded.

The peel strength value can be used to evaluate whether sufficient adhesion has occurred with a larger force indicating stronger adhesion. In Figure 5.21, the peel strengths of a standard Na-AMPS hydrogel manufactured by First Water (Ramsbury, Wiltshire, UK) on skin and on the smooth stainless steel surface are compared, also using the modified Hounsfield Tensometer in Figure 5.19. This comparison, which shows the peel strength on stainless steel to be 3-4 times higher than on skin, demonstrates the sensitivity of the testing procedure to the nature of the substrate.

Thickness (mm)	**Width (mm)**	**Max Force (N)**	**Max Force/Width (N/mm)**

1.20	25.00	2.010	0.0804

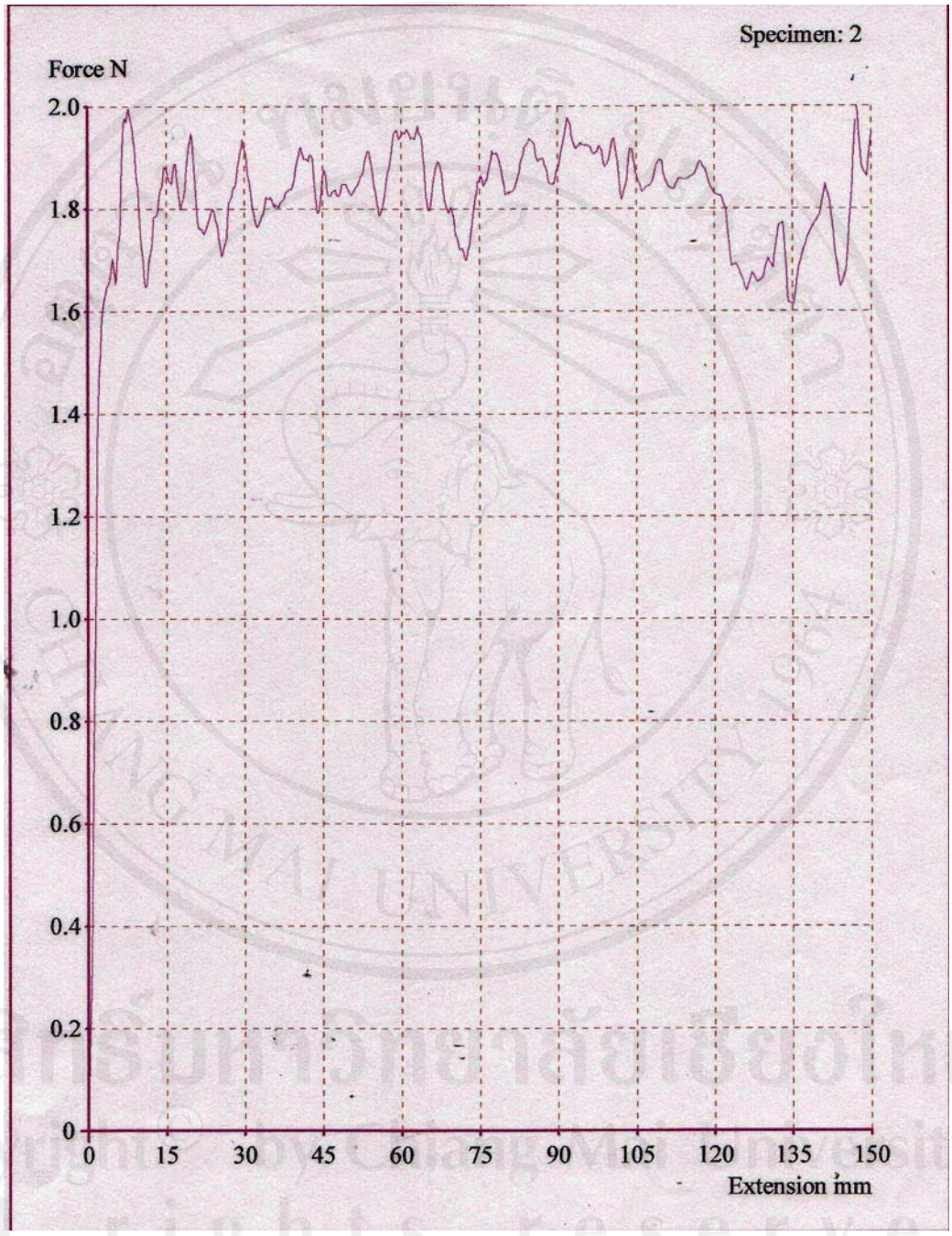

Figure 5.20: Peel test data for the System I Na-AMPS hydrogel on human skin (author's forearm) from the modified Hounsfield Tensometer.

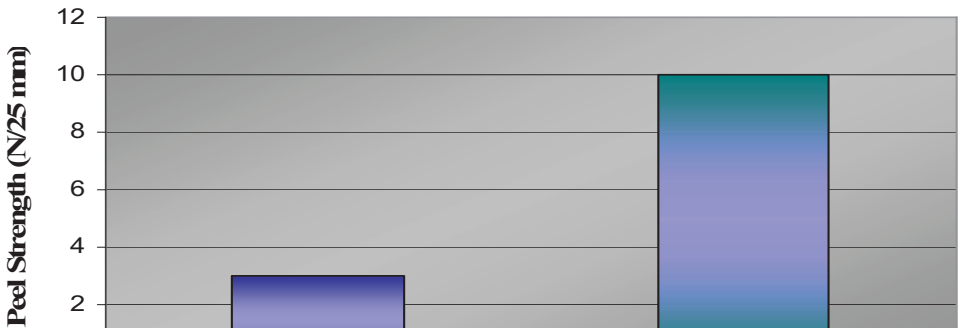

Figure 5.21 : Comparison of the average 90° peel test results for a standard Na-AMPS hydrogel (First Water) on different substrates [90].

The peel strengths from the skin of the System I and II hydrogels are shown in Figure 5.22 alongside a commercial skin adhesive hydrogel (used for an ECG electrode) for comparison. There was no significant difference in their peel strengths which was not surprising since whatever differences there may have been in their crosslinking would not have been expected to seriously affect their peel strengths. Adhesive strength, and therefore peel strength, is more dependent on a material's surface properties than its bulk properties since it is the adhesive bond between the sample surface and the substrate which is the dominant factor. Since the System I and II hydrogels have the same surface composition, both incorporating strong ionic and hydrogen bonding interactions, their peel strengths are very similar as would be expected.

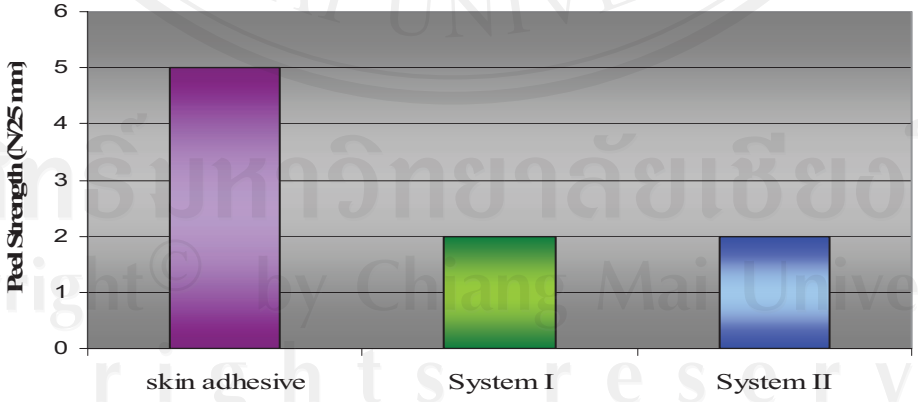

Figure 5.22 : Peel strengths of System I and System II Na-AMPS hydrogels from skin compared with a commercial skin adhesive material.

As regards their actual skin adhesion, both hydrogels showed good adhesion to healthy skin without being so strongly adhesive as to be painful to remove. The series

of photographs below in Figure 5.23 for the Series II hydrogel illustrate its ease of application, good skin adhesion, and ease of removal. In the case of its application to a wound surface, its removal can be facilitated by spraying with water (or aqueous antiseptic solution) in order to minimize the detachment of new epidermal cells (stripping effect) as previously mentioned.

(a) ease of application

(b) good skin adhesion

(c) ease of removal

Figure 5.23 : Photographs of the System II hydrogel sheet on healthy skin.

5.3.2.5 Oxygen Permeability [109-113]

Most methods of oxygen permeability determination use either gravimetric (change in sample weight), barometric (change in ambient gas pressure), or volumetric (change in ambient gas volume) measurements. These methods quantify gas sorption into or desorption out of a polymer sample or gas permeation through a polymer membrane. Current commercial instruments often rely on modern thermal conductivity, coulometric, or ionisation-based detectors.

Ng et al. [109] studied the dissolved oxygen permeability of poly(2-hydroxyethyl methacrylate), poly(HEMA), hydrogels used in contact lens applications. The oxygen permeability through this lens material was shown to be insufficient on its own to preserve corneal transparency and a fresh tear fluid layer behind the lens was necessary for the lens to be suitable for daily wear. Poly(HEMA) lenses were also shown to be unsuitable for continuous wear. It was found that the permeability of dissolved oxygen through hydrogels is approximately an exponential function of the equilibrium water content over a wide range of water contents. However, chain flexibility, water-binding ability and pore size distribution, particularly at low water contents, also affect oxygen permeability.

Corkhill et al. [110] and Ng and Tighe [109] reported that the dissolved oxygen permeability (Pd) of a hydrogel is governed by its equilibrium water content (EWC) at an EWC of around 30% and above, as given by the equation :

$$Pd = 24 \times 10^{-10} e^{0.0443\ EWC} \qquad (5.3)$$

where

Pd = dissolved oxygen permeability (ml (STP) mm)/(cm^2.s.cmHg)
EWC = equilibrium water content of the hydrogel (%)
STP = standard temperature and pressure (25°C, 760 mmHg)

The validity of this equation was demonstrated by the linearity of the semi-log plots in Figure 5.24.

Figure 5.24 : Approximately linear dependence of log Pd on equilibrium water content for various hydrogels at 25°C (○) and 34°C (●) [109].

The main problems associated with hydrogels of high water content, such as the Na-AMPS hydrogels prepared in this work, are the progressive decrease in strength and increase in linear and volume swell as the water content increases. While increasing water content is advantageous for oxygen permeability, there will be, for a given class of polymer, a point beyond which further increase in water content no longer provides a net gain in oxygen permeability. Thus, for a given thickness of dehydrated polymer, a point is reached in terms of increasing water content when the increase in linear swell is greater than the increase in oxygen permeability coefficient [112-114].

In this work, oxygen permeability measurements were carried out using a Permiometer Model 201T, as shown in Figure 5.25, in conjunction with a chart plotter.

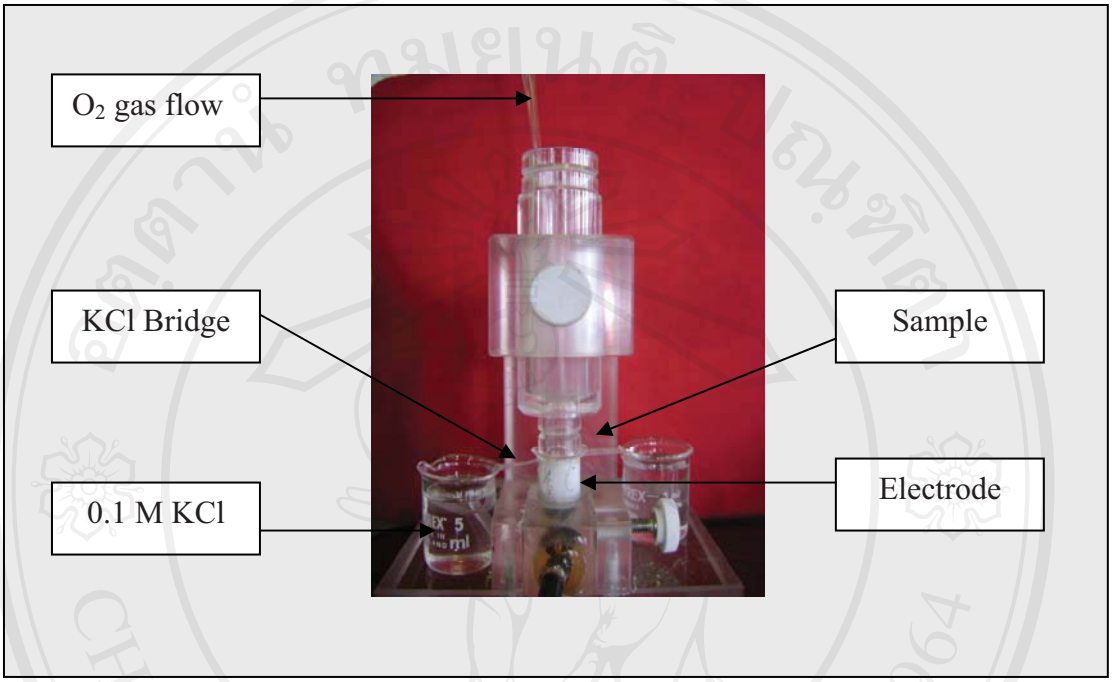

Figure 5.25: Permiometer Model 201T used for oxygen permeability measurements.

Hydrogel samples were cut to size using a size 7 cork borer and the thickness (0.10 ± 0.02 mm) measured using a micrometer. Each sample was placed over an electrode with a lens tissue saturated in 0.1 M potassium chloride (KCl) as an electrode bridge in between the sample and the electrode. A column was then placed over the sample, as shown in Figure 5.25, and a constant stream of N_2 gas passed through the sample until a steady current was obtained. This steady current was then recorded as i_0. In all cases, i_0 in this study was found to be zero, signifying that there was no O_2 gas in the system before measurement. Then, O_2 gas was introduced into the system and the new steady current reading obtained recorded as i. The oxygen permeability (Dk) was calculated using equations (5.4) and (5.5). The value of Dk is a measure of both the solubility of O_2 in a material and the diffusivity of O_2 through the material.

$$Dk = L(i - i_0)\, V / n\, F\, A\, P_s \qquad (5.4)$$

where

L	=	sample thickness (mm)		
i_0	=	current obtained for N_2 gas	=	0 (in all cases)
i	=	current obtained for O_2 gas		
F	=	Faraday constant	=	96490 x 10^6 μA.s.mol^{-1}
A	=	area of gold electrode	=	0.1278 cm^2
P_s	=	oxygen pressure	=	760 mmHg (STP)
n	=	number of electrons involved	=	4
V	=	standard gas molar volume	=	22.415 x 10^3 ml

If the various constants are calculated, this equation (5.4) reduces to:

$$Dk = i\,(\mu A) \times L\,(mm) \times (6 \times 10^{-11}) \quad (cc.mm./cm^2.s.mmHg) \qquad (5.5)$$

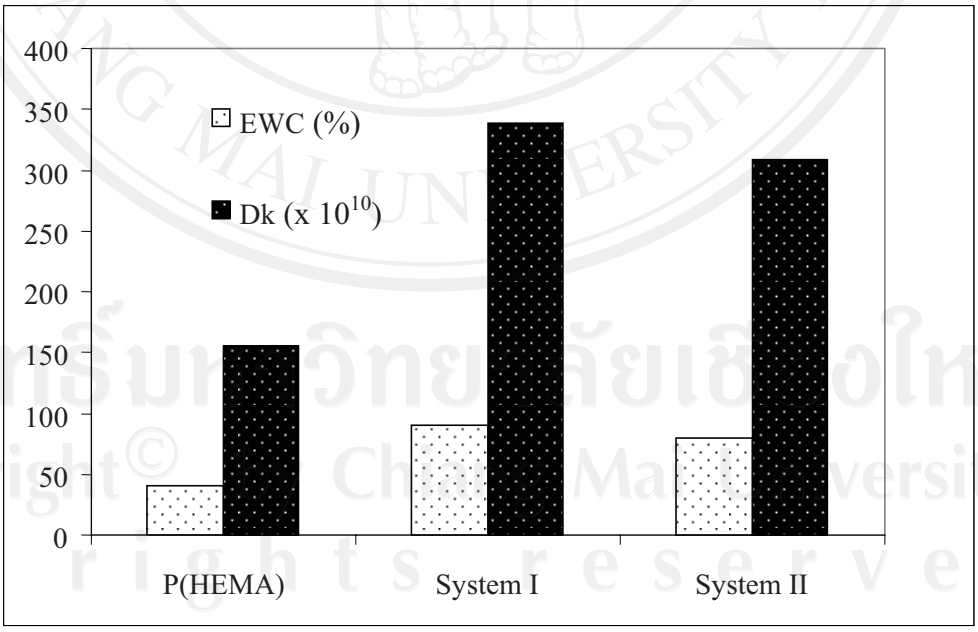

Figure 5.26 : Oxygen permeabilities (Dk) and corresponding equilibrium water contents (% EWC) of the Na-AMPS System I and System II hydrogel sheets compared with poly(HEMA).

It was found that the Dk values of the Na-AMPS hydrogel sheets were about 300 x 10^{-10} - 350 x 10^{-10} cc.mm./cm^2.s.cmHg, significantly higher than polyHEMA for which the Dk is about 150 x 10^{-10} cc.mm./cm^2.s.cmHg [109]. As shown in Figure 5.26, these Dk values correspond to the respective equilibrium water contents. Thus, from the point of view of oxygen permeability, the high Dk values of the Na-AMPS hydrogels are advantageous for their use as wound dressings since they would readily allow oxygen exchange to and from the wound surface. This oxygen exchange allows the wound to "breathe" which, in turn, aids the wound healing process.

The mechanism by which the water content of the hydrogel facilitates oxygen permeability is simplistically represented in Figure 5.27. In a Na-AMPS hydrogel, the relatively large SO_3^- sulfonate anion is strongly interactive with the adjacent water molecules which then become "bound water". By shielding the ionic charges, this then allows the network to expand, thereby allowing the "free water" molecules to solubilize the oxygen molecules and transport them through the hydrogel matrix.

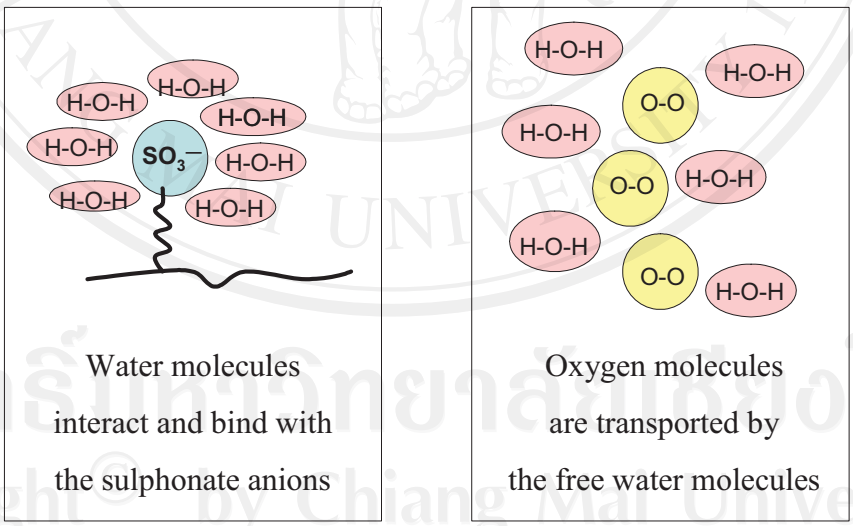

Figure 5.27 : Simplified representation of (a) water solubilization of the SO_3^- groups and (b) oxygen transport by the free water molecules in a Na-AMPS hydrogel.

5.3.2.6 Residual Monomer [115-117]

Due to the equilibrium nature of polymerisation reactions, even though they may be heavily weighted thermodynamically in favour of polymer formation, there will always be a small amount of residual monomer (= the equilibrium monomer concentration) remaining in the system at the end of the reaction. This residual monomer, unlike the polymer, is usually toxic to the human body to at least some extent and therefore needs to be kept to the absolute minimum amount possible if not removed completely.

In this study, residual Na-AMPS monomer in the System I and II hydrogels was determined by ion chromatography. Ion chromatography (IC) is an analytical technique which involves separating and quantifying anions and cations using liquid chromatography (LC). The sample containing the ions dissolved in a suitable solvent is injected into a column which contains a stationary phase with a surface of opposite charge to the sample ions. The stronger the charge on the sample, the stronger its attraction to the ionic surface and the longer it takes to elute. Both the pH and the ionic strength of the mobile phase control the elution time. Once the ions are separated, they are detected and quantified by a conductivity detector.

For the System I and II hydrogels, the residual Na-AMPS monomer was first extracted by immersion in distilled and deionised water for 24 hrs. For calibration purposes, standard solutions of Na-AMPS in water of 0.01, 0.05, 0.10, 0.25, 0.50 and 1.00 % w/v were prepared. The IC instrument used was a Dionex DX600 Ion Chromatograph supported by Chromeleon Client 6.50 software, as shown in Figure 5.28. The eluent used was 5 mM aqueous potassium hydroxide (KOH) solution over an analysis time of 40 mins.

Both the hydrogel extracts and the standard solutions were arranged in the ion chromatograph for autosampling as shown in Figure 5.29. The instrument was set up for analysis of the residual sulfonate SO_3^- anions in the sample via the sequence of operations shown in the schematic diagram in Figure 5.30. The linear calibration plot of elution peak area against Na-AMPS concentration for the Na-AMPS standard

solutions from the data in Table 5.11 is shown in Figure 5.31. When the results for the hydrogel extracts, shown in Figures 5.32 and 5.33, were compared with the calibration plot, residual Na-AMPS monomer contents of 0.15% and 0.01% w/v were obtained for the System I and System II hydrogels respectively.

These residual monomer contents of 0.15% and 0.01% w/v are low by general polymerisation standards, which is advantageous for a wound dressing. This indicates that the photopolymerisation method of synthesis and the two photoinitiators used (ACPA and Irgacure 184) are highly efficient for the polymerisation of Na-AMPS under the conditions used. This is especially true of the System II photoinitiator, Irgacure 184, which gave a residual monomer content of an order of magnitude less than ACPA. While any residual monomer, however small, is still a cause for concern, it may be noted here that γ–irradiation, which is normally used in the sterilization process for a hydrogel wound dressing, would be expected to further reduce if not eliminate completely this residual monomer.

Table 5.11: Peak area and Na-AMPS concentration data from ion chromatography for the Na-AMPS standard solutions and the System I and II hydrogel extracts.

SAMPLE	PEAK AREA * µs/min	[Na-AMPS] % w/v
STANDARD SOLUTIONS		
0.01% w/v Na-AMPS	1.25	0.01
0.05% w/v Na-AMPS	2.50	0.05
0.10% w/v Na-AMPS	7.50	0.10
0.25% w/v Na-AMPS	12.50	0.25
0.50% w/v Na-AMPS	37.50	0.50
1.00% w/v Na-AMPS	75.00	1.00
HYDROGEL EXTRACTS		
System I hydrogel	11.60	0.15
System II hydrogel	1.61	0.01

* Average of 3 readings

Figure 5.28 : Dionex DX600 Ion Chromatograph supported by Chromeleon Client 6.50 software used for residual monomer determination.

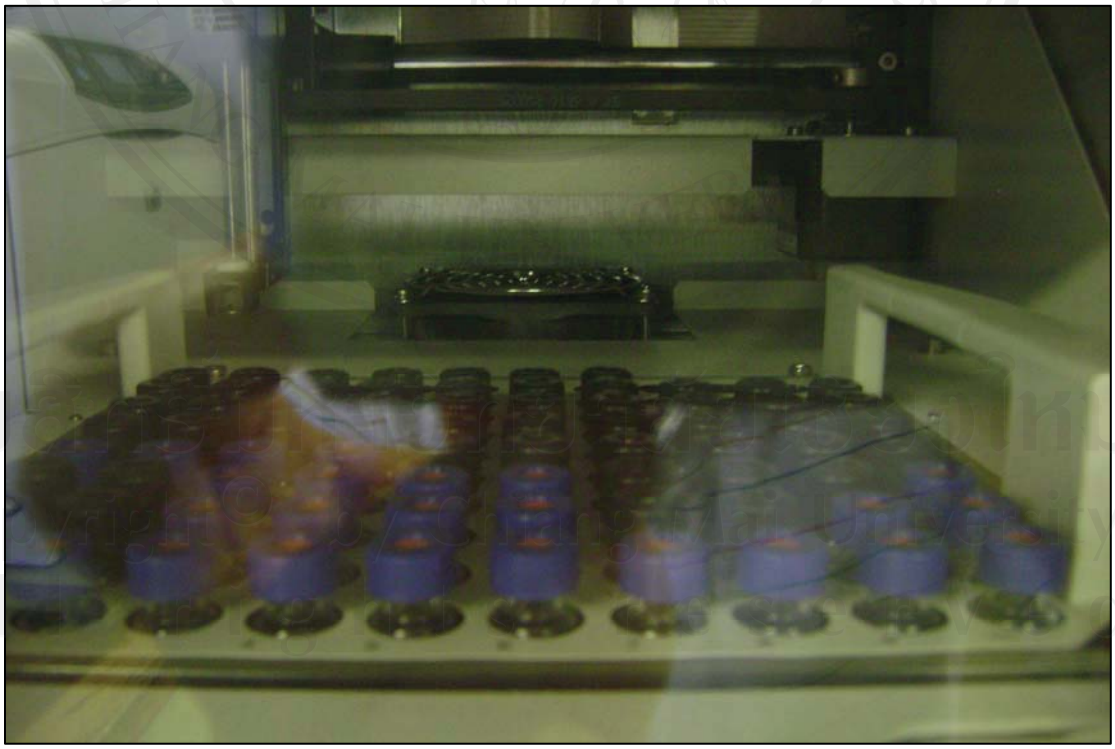

Figure 5.29: Sample arrangment in the ion chromatograph for autosampling.

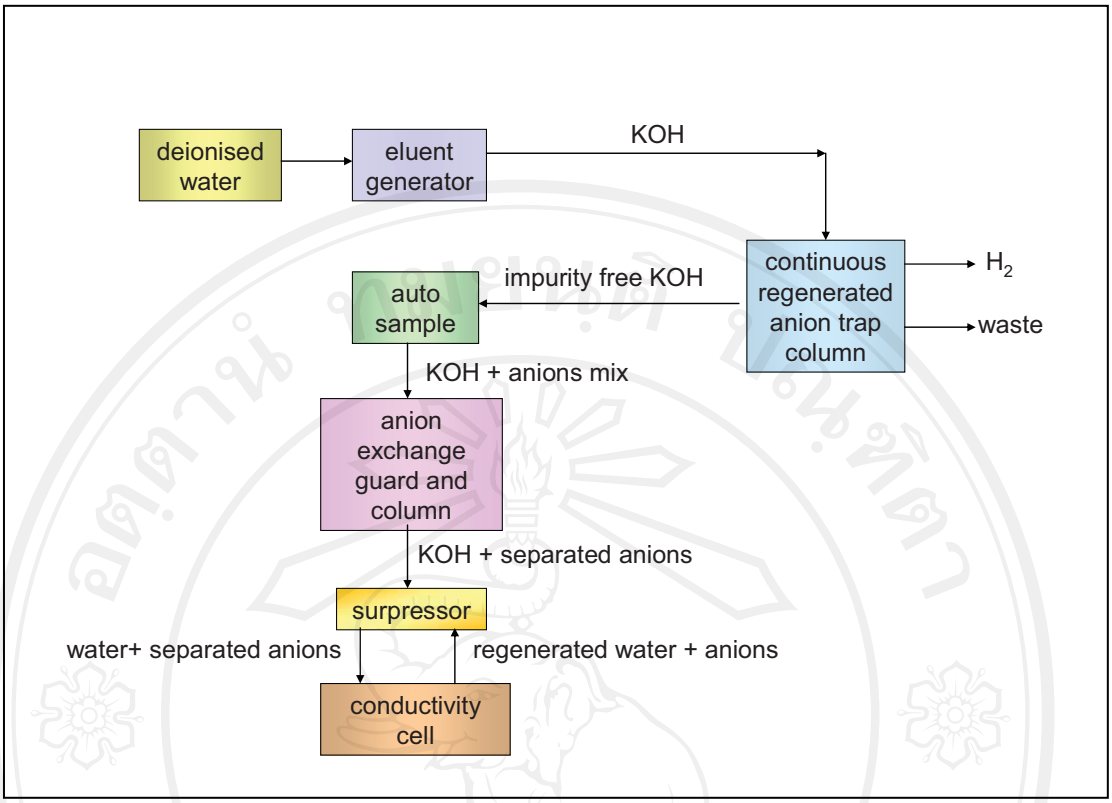

Figure 5.30 : Schematic diagram of the Dionex DX600 Ion Chromatograph.

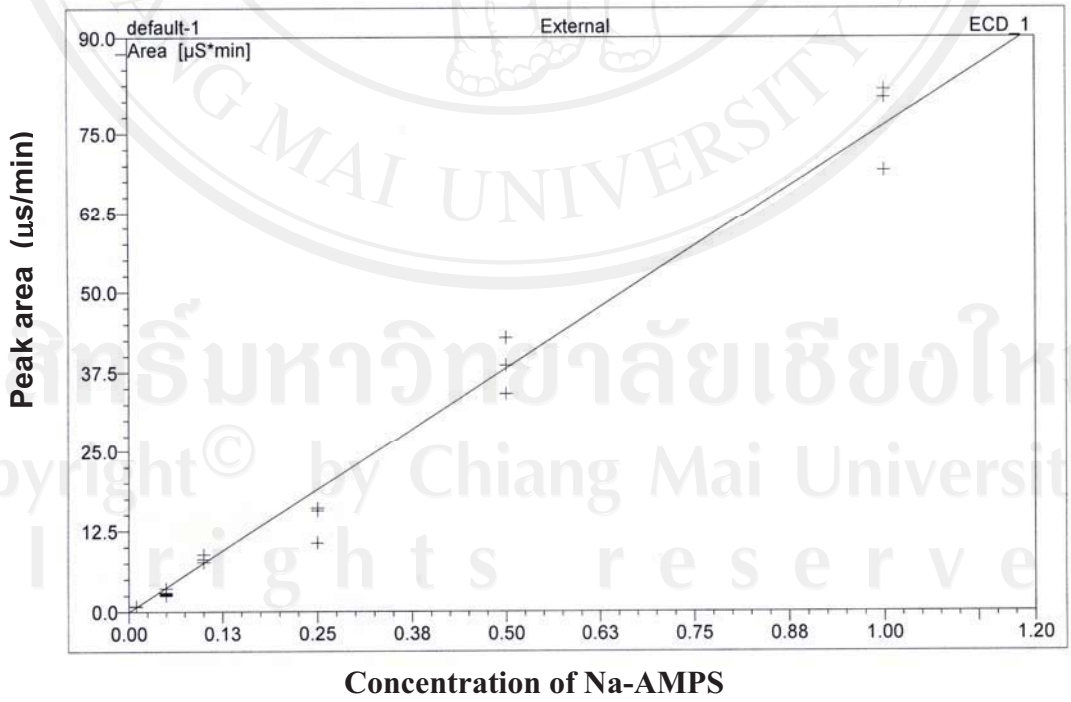

Figure 5.31 : Calibration plot of concentration (% w/v) of the standard Na-AMPS solutions against peak area (µs/min) from ion chromatography.

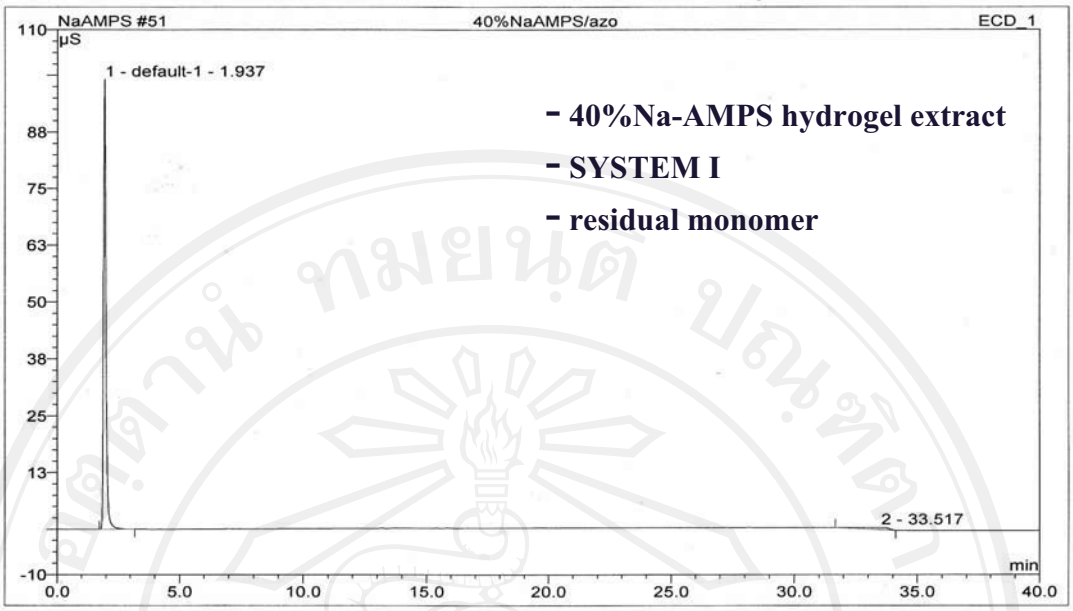

No.	Ret.Time min	Peak Name	Height µS	Area µS*min	Rel.Area %	Amount	Type
1	1.94	default-1	99.103	11.591	95.25	n.a.	BMB
2	33.52	n.a.	0.458	0.578	4.75	n.a.	BMB
Total:			99.562	12.169	100.00	0.000	

Figure 5.32 : IC chromatogram of the Na-AMPS System I hydrogel's residual SO_3^- anions.

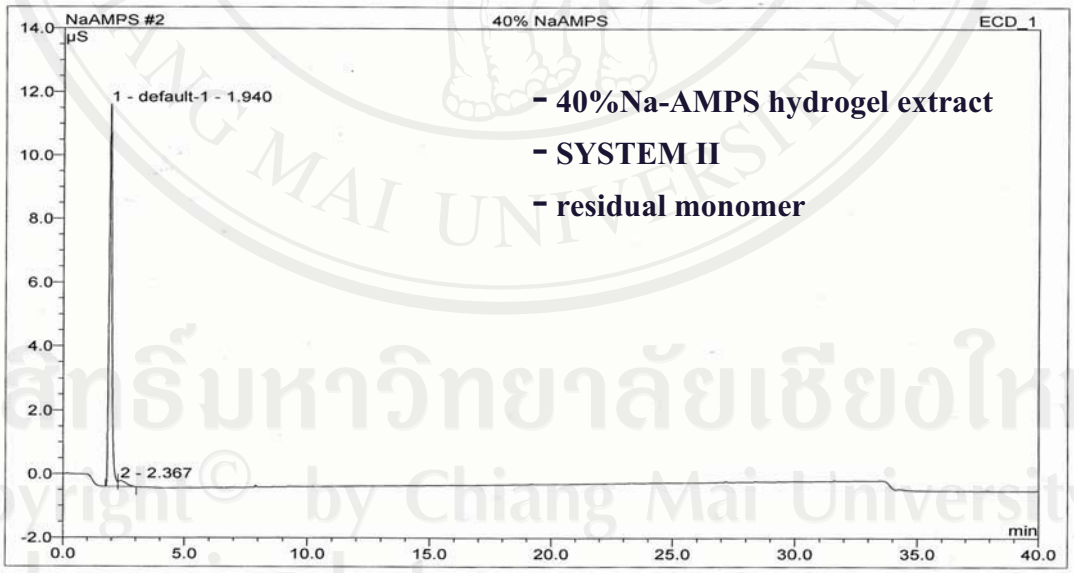

No.	Ret.Time min	Peak Name	Height µS	Area µS*min	Rel.Area %	Amount	Type
1	1.94	default-1	12.010	1.610	95.69	n.a.	BM
2	2.37	n.a.	0.195	0.073	4.31	n.a.	MB
Total:			12.205	1.682	100.00	0.000	

Figure 5.33 : IC chromatogram of the Na-AMPS System II hydrogel's residual SO_3^- anions.

5.3.2.7 Cytotoxicity Testing [118-120]

Cytotoxicity is simply defined as the quality of being toxic to cells. Examples of toxic agents are a chemical substance, an immune cell or some type of venom. Treating cells with a cytotoxic compound can result in a variety of cell fates. The cells may undergo necrosis in which they lose membrane integrity and die rapidly as a result of cell lysis. Alternatively, the cells can stop actively growing and dividing (a decrease in cell viability) or the cells can activate a genetic program of controlled cell death (apoptosis). Thus, cytotoxicity testing is a necessary part of the overall testing procedure for any material that is to be used in a biomedical application which involves direct contact with living tissue.

In the experiments carried out here, the Na-AMPS hydrogel sheet samples were first sterilized by γ-irradiation prior to cytotoxicity testing with L929 cells (mouse fibroblasts) by the direct contact method. High-density polyethylene (HDPE) and natural rubber containing carbon black were used as negative and positive controls respectively. These tests were carried out in the Cell Culture Unit of the National Metal and Materials Technology Center (MTEC).

The substances used were:

(1) mouse fibroblasts, ECACC No. 85011425, cell concentration = $6x10^4$ cells/disc
(2) Dulbecco's Modified Eagle's Medium (DMEM) with 10% (v/v) fetal bovine serum, L-glutamine, penicillin (100 units/ml) and streptomycin (100 μg/ml) (Gibco ™, Paisley, UK) for fibroblast culture
(3) non-toxic dental wax with 1 mm diameter and 15 mm length
(4) phosfate buffer saline (PBS) pH 7.4
(5) 0.01% v/v neutral red in phosfate buffer saline

Hydrogel test specimens were cut into small square pieces 1 x 1 cm in size and saturated with growth medium. The samples were placed in the middle of a 35 mm dish and fixed with non-toxic dental wax. L929 cells were then seeded into the dish at a density of $6x10^4$ cells/dish and incubated for 48 hrs at 37°C. Cell morphology and

the toxic zone were evaluated by inverted phase contrast light microscopy after the 48 hrs exposure to the cells. The cells were stained with 0.01% neutral red in phosfate buffer saline (PBS) for membrane integrity. Finally, the samples were gold sputtered under vacuum and examined microscopically using a Jeol JSM-5410 Scanning Electron Microscope to observe the cellular morphology and behaviour of the L929 cells on the samples. Each sample was tested in triplicate and the tests repeated twice.

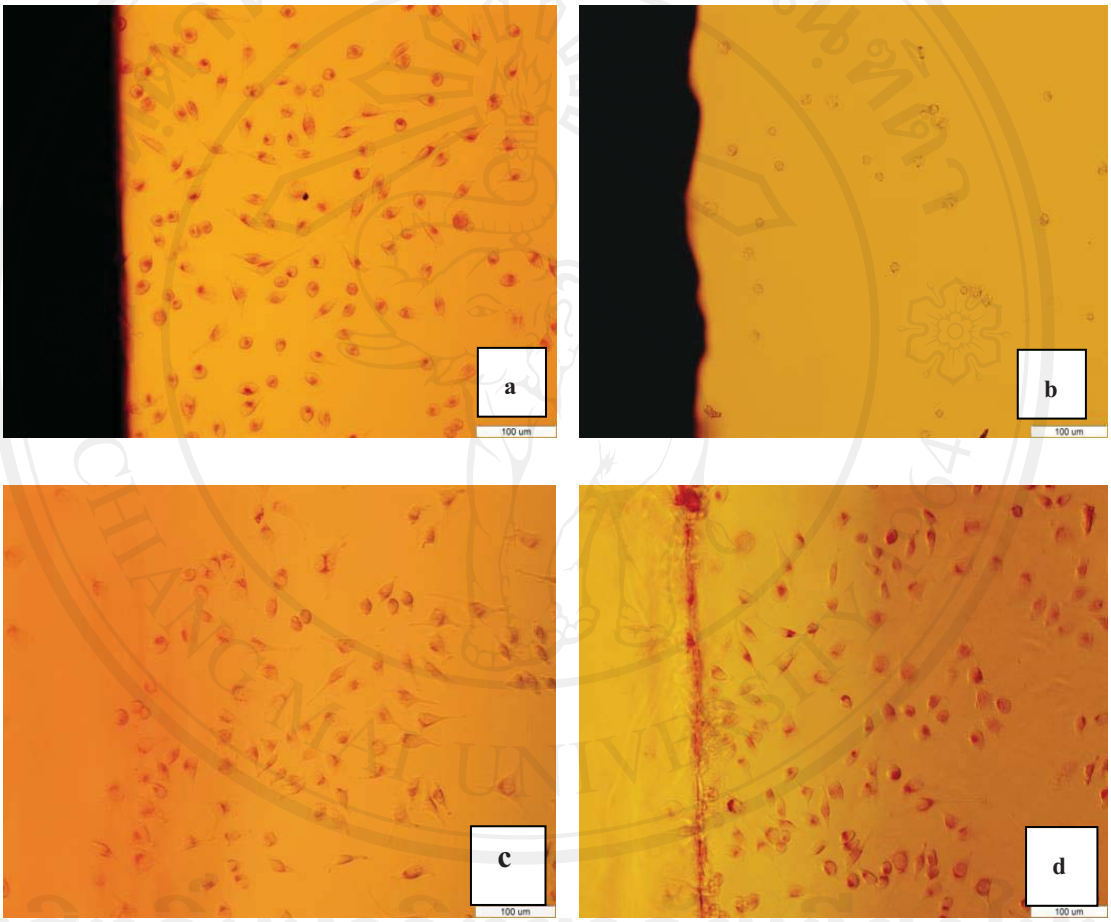

Figure 5.34 : Scanning electron micrographs (magnification x 200) showing the L929 cells after cytotoxicity testing for 48 hrs at 37°C on the following substrates :

(a) HDPE (negative control)

(b) natural rubber containing carbon black (positive control)

(c) System I Na-AMPS hydrogel

(d) System II Na-AMPS hydrogel

As the SEM results in Figure 5.34 show, both the System I and System II hydrogels are clearly non-toxic since they exhibited similar cell responses to the HDPE negative control. This similarity extended to both cell viability (number) and morphology (size and shape). While this may not be a new finding in itself, since Na-AMPS hydrogels have already found commercial use in wound dressings, what it does show, and which is important to this present work, is that any residual traces of monomer (also photoinitiator and crosslinker) still present in the hydrogels from the synthesis reactions were of a sufficiently low level not to cause cytotoxity. This is consistent with the previous residual monomer measurements from ion chromatography and would have been further aided by the γ–ray sterilization process carried out prior to cytotoxicity testing.

5.4 Effect of Humectant

Although the main factor determining the properties of a hydrogel is obviously the polymer's chemical structure, including any crosslinking, the properties can be modified to some extent by the addition of other chemical substances (additives). An example of this is the addition of what is called a ***humectant***.

A humectant is a hygroscopic compound through its affinity to form hydrogen bonds with and/or be solubilized by water molecules and is therefore often a compound which contains hydroxyl groups. Humectants find use as food additives to keep food moist and as moisturizers in a wide range of cosmetic and healthcare products. In the case of a wound dressing, the role of a humectant is primarily to interact (i.e., bind) with the free water and thereby decrease its loss from the hydrogel network, both in terms of amount and rate. In this way, the humectant, which itself remains in the hydrogel, ensures that the hydrogel remains moist and flexible in contact with the wound surface and does not "dry out" as some hydrogel dressings might otherwise do.

In this work, 2 different humectants were compared, namely:

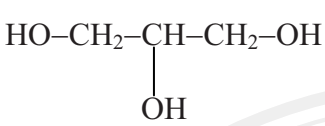

glycerol
(Gly)
slightly viscous liquid

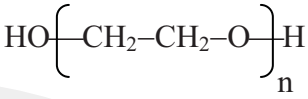

poly(ethylene glycol) 10000 ($\bar{n} \approx 220$)
(PEG)
waxy solid (m.pt. = 62-65°C)

The humectant concentrations used were :

Gly : 10, 20 and 30% by weight
PEG : 5, 10 and 15% by weight

as shown in Table 5.12 below. The humectant was added in place of an equivalent part of the water in the synthesis of the 40% Na-AMPS System II (only) hydrogel sheets.

Table 5.12 : 40% Na-AMPS System II hydrogel formulations used to study the effects of the humectants glycerol (Gly) and poly(ethylene glycol) 10000 (PEG).

SAMPLE CODE	COMPOSITION (% by weight) *		
	Na-AMPS	WATER	HUMECTANT
Gly-10	40	50	10
Gly-20	40	40	20
Gly-30	40	30	30
PEG-5	40	55	5
PEG-10	40	50	10
PEG-15	40	45	15

* not including the Irgacure 184 (photoinitiator) and Ebecryl 11 (crosslinker)

Gly = glycerol

PEG = poly(ethylene glycol) 10000

The hydrogel sheets incorporating the humectant were prepared as described in the previous chapter. Both glycerol and PEG are widely used as humectants since they can hydrogen-bond with (in the case of glycerol) and/or be solubilized by (in the case of PEG) many water molecules. PEG tends to be preferred since it is readily available in a wide range of molecular weights ($\overline{M}_n \approx$ 200-20,000) and, being a polymer, is less likely to leach out. The intercalation of the glycerol and PEG humectant molecules in the crosslinked Na-AMPS hydrogel network is represented in Figure 5.35 below.

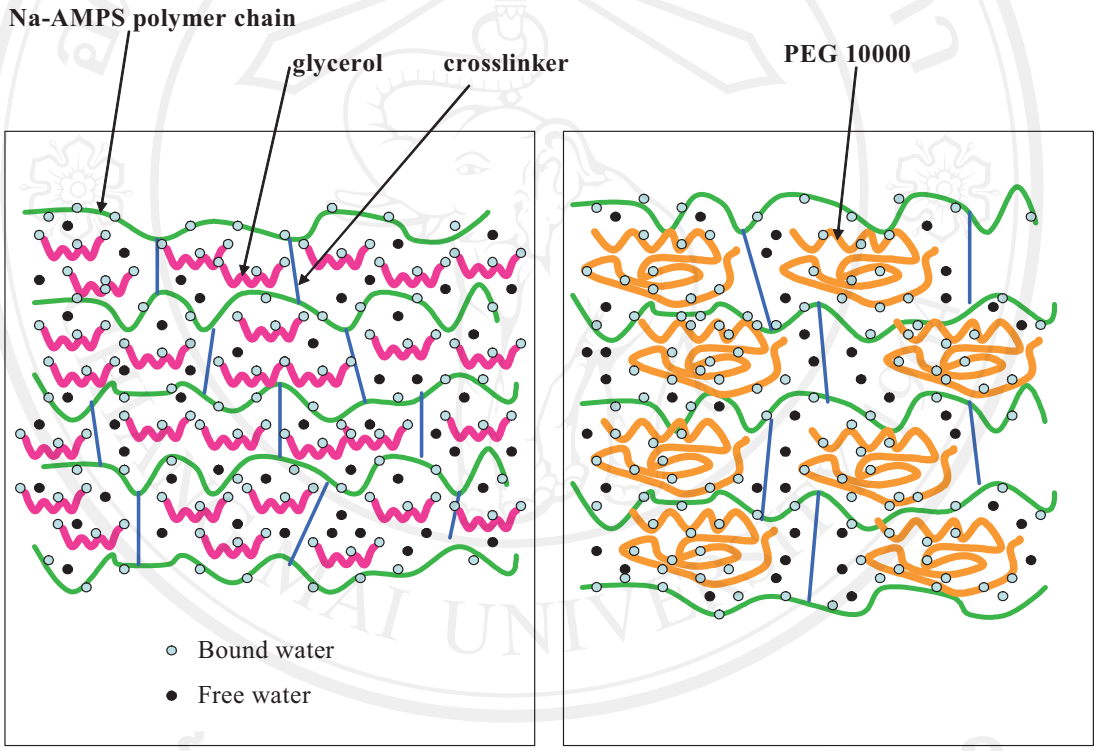

Figure 5.35 : Intercalation of glycerol and PEG as humectants in a crosslinked Na-AMPS hydrogel network.

The effects of the glycerol and PEG humectants at the same 10% by weight concentration are shown in Figures 5.36-5.38 for

- water absorption
- water retention
- water vapour transmission

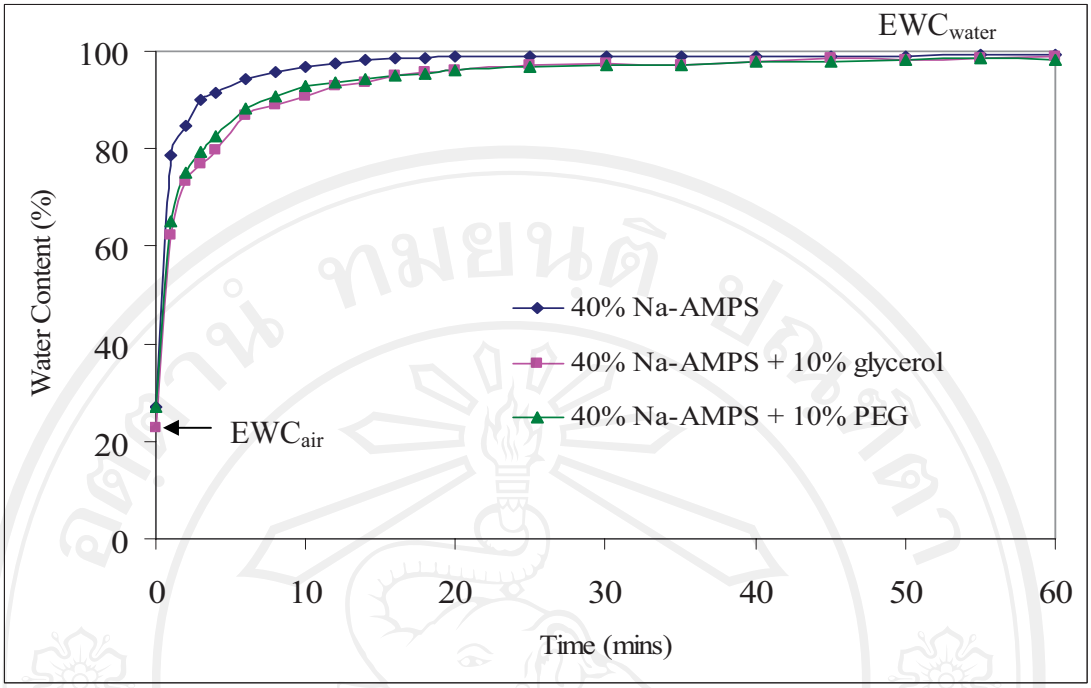

Figure 5.36 : Water absorption – time profiles for Na-AMPS hydrogel sheets in distilled water at 37°C showing the effects of adding 10% by weight of glycerol and PEG 10000 as humectants.

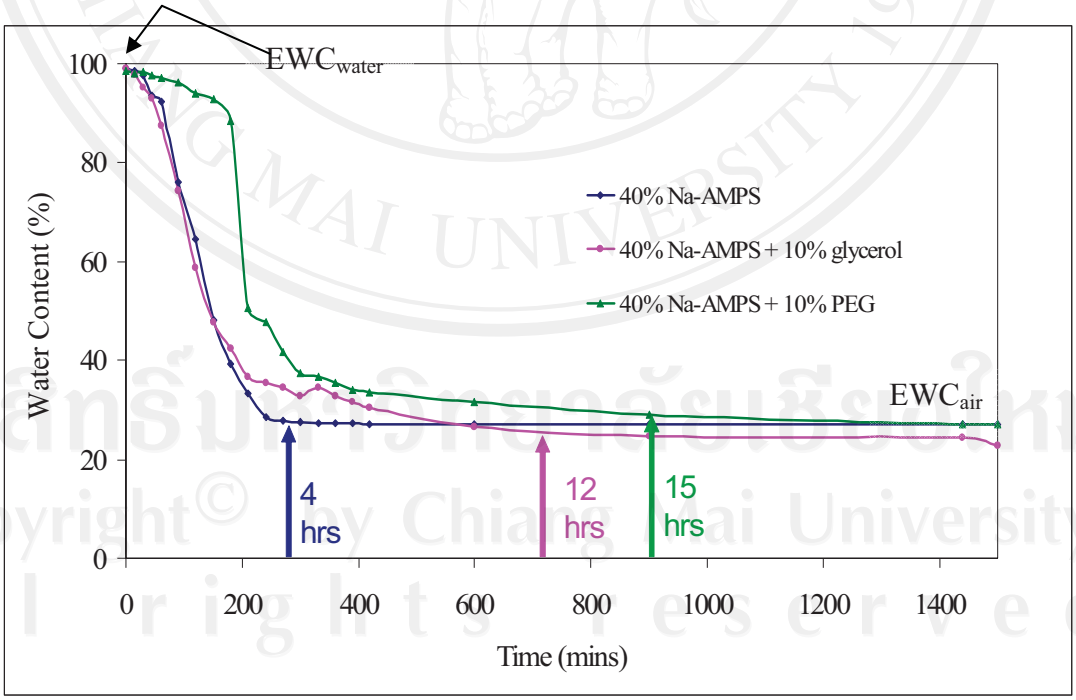

Figure 5.37 : Water retention – time profiles for Na-AMPS hydrogel sheets in air at room temperature showing the effects of adding 10% by weight of glycerol and PEG 10000 as humectants.

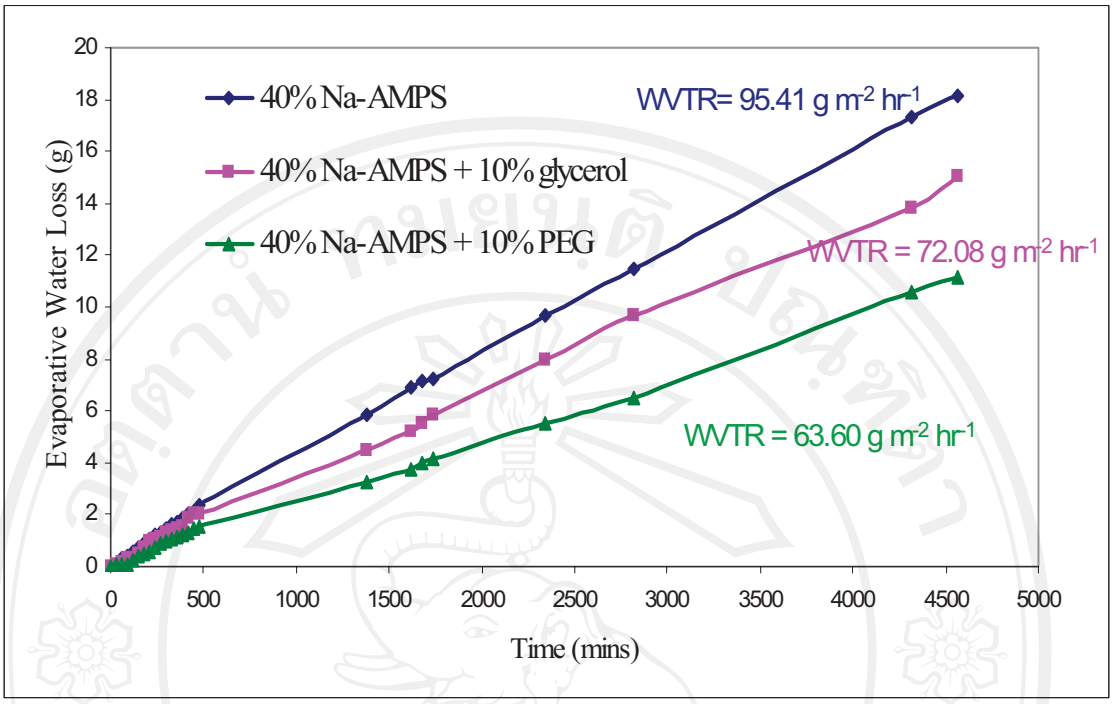

Figure 5.38 : Water vapour transmission rates (WVTR) for Na-AMPS hydrogel sheets at 37°C showing the effects of adding 10% by weight of glycerol and PEG 10000 as humectants.

The water absorption profiles in Figure 5.36 show that glycerol and PEG at the 10% by weight level have relatively little effect except to slow down slightly the approach to EWC. Their effects are more noticeable, especially for PEG, in slowing down the rate of water loss in the water retention profiles in Figure 5.37. However, it is significant to note that both the glycerol and PEG only affected the rate of water loss, not the amount since the final EWC_{air} was approximately the same with and without humectant. The most noticeable change is the decrease in WVTR, as shown above in Figure 5.38, with PEG again being more effective than glycerol. This decrease in WVTR can be explained in terms of the humectant binding some of the free water (PEG > glycerol), thereby decreasing the rate of water transport through the hydrogel, as depicted previously in Figure 5.17 on page 89.

The effects of humectant concentration on peel strength and oxygen permeability are demonstrated in Figures 5.39 and 5.40. In Figure 5.39, both humectants decrease peel strength significantly, more so with increasing concentration. This can be interpreted in terms of the humectant maintaining a lubricating layer at the hydrogel-substrate interface. This in turn weakens the adhesive force between the hydrogel and the substrate resulting in a decrease in peel strength. These molecular effects at the microscopic level are reflected at the macroscopic level as a slightly oily surface feel to the humectant-containing hydrogels, especially at the higher concentrations. In this way, the humectant molecules, whether glycerol or PEG, which migrate to the hydrogel surface can be visualized as forming a lubricating layer of humectant together with bound and/or solubilizing water molecules. Thus, in addition to its desired effect of helping to retain water within the hydrogel, the humectant can also have less desirable side-effects such as loss of skin adhesion. These peel strength tests were carried out as described previously using the modified Hounsfield Tensometer.

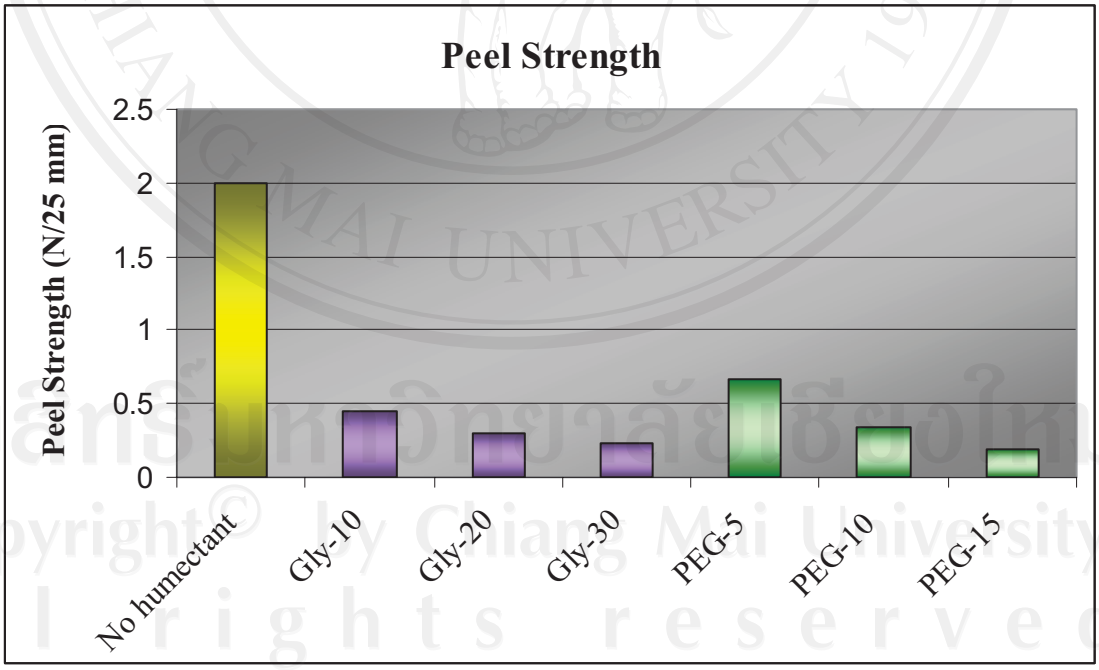

Figure 5.39 : Effects of humectant addition and concentration on the peel strength of the System II Na-AMPS hydrogel.

The effect of humectant concentration on oxygen permeability (Dk), as shown in Figure 5.40, is both complicated by the test conditions and masked by the humectant's effect on water content which, as mentioned previously, is an important determinant of Dk. In the oxygen permeability test, the sample comes into contact with an aqueous potassium chloride (KCl) solution which swells the sample to varying extents depending on composition. As the results in Figure 5.40 below show, the Dk values tend to follow the same trends as the water contents. In the case of glycerol, the Dk value increases with the glycerol concentration whereas, in the case of PEG, it appears to decrease. The reason(s) for this difference is unclear but it is obviously related in some way to the water content. One possibility is that the glycerol molecules, being small individual molecules which can move around inside the hydrogel network much more easily than the longer chain PEG molecules, allow oxygen molecules to be transported through the hydrogel by the free water at a faster rate due to the higher molecular mobility. However, this is taking a rather simplistic view of what is a complex balance of interrelated factors. Further studies are required before firmer conclusions can be drawn.

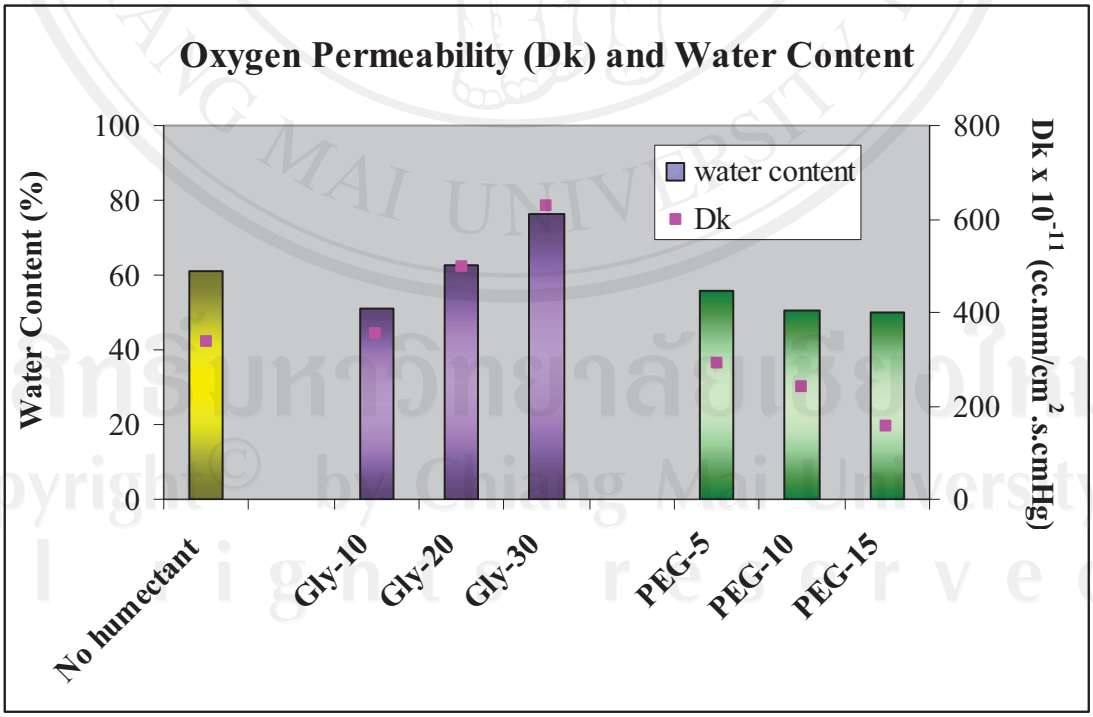

Figure 5.40 : Effects of humectant addition and concentration on the oxygen permeability of the System II Na-AMPS hydrogel sheets.

5.5 Mechanical Strength Improvement and Multilayer Construction

One of the main shortcomings of hydrogel sheets in their application as wound dressings is their loss of mechanical strength as they become hydrated. Crosslinking can help but, if the hydrogel has a very high EWC, such as the Na-AMPS hydrogels studied here, even crosslinking only brings about a limited improvement in, for example, tear strength.

As the final part of this property section of the thesis, the use of a ***reinforcing polymer mesh*** was investigated as a means of improving the cohesive strength of the hydrogel, especially when hydrated, without compromising its other properties. Various cloth-like meshes are readily available commercially as domestic products (e.g., curtain meshes) made from materials such as cotton, polyester (PET), nylon and polyethylene. The chosen mesh was inserted into the middle of the hydrogel sheet during the polymerisation step inside the mould so that the Na-AMPS monomer in aqueous solution polymerised around it. After its removal from the mould, one side of the sheet was covered with an adhesive polyurethane (PU) film as a backing sheet and the other side with a poly(ethylene terephthalate) (PET) film as a release liner, as shown in Figure 5.41. A photograph of the polyethylene mesh-reinforced System II hydrogel sheet is shown in Figure 5.42 alongside that of a commercial 'Second Skin' (Spenco Medical (UK) Ltd.) hydrogel wound dressing upon which the mesh-reinforcement and multilayer construction was modeled. 'Second Skin' is a γ–ray-crosslinked poly(ethylene oxide)-based hydrogel.

Qualitative observations of the effectiveness of the mesh showed that it was indeed effective in providing a internal scaffold for holding the hydrogel together as it swelled on hydration. However, since the mesh itself did not swell, its effectiveness a as a reinforcement appeared to be limited to moderate water contents at which the volume expansion of the hydrogel was not too high.

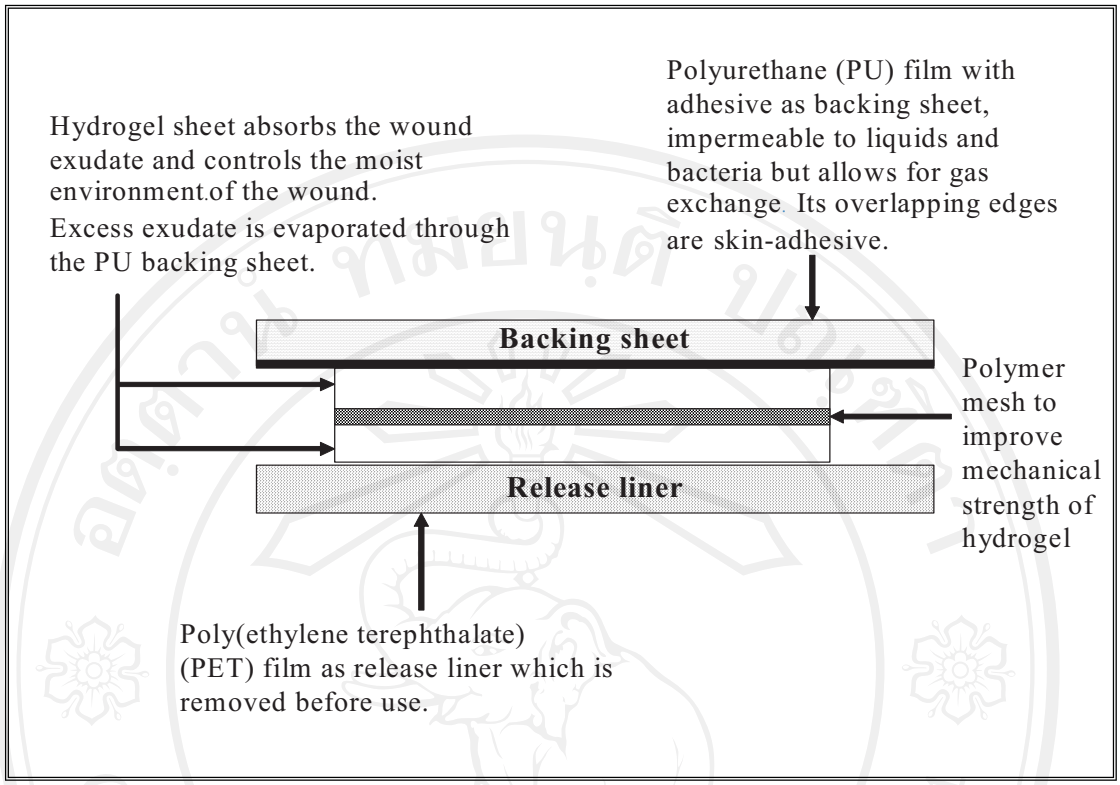

Figure 5.41: Mesh-reinforced Na-AMPS hydrogel sheet showing its multilayer construction as a prototype wound dressing.

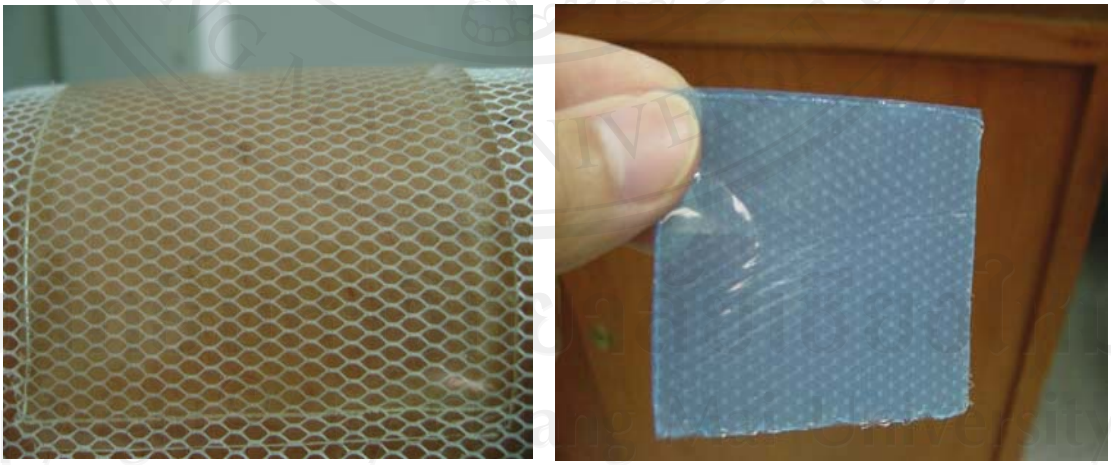

(a) (b)

Figure 5.42 : Photographs showing (a) the polyethylene mesh-reinforced Na-AMPS System II hydrogel sheet, as obtained direct from photopolymerisation in the mould, compared with (b) a commercial 'Second Skin' wound dressing.